Other Tumors of the Cervix (Melanocytic, Germ Cell, Trophoblastic, Lymphoid, and Myeloid Tumors)

12

Gulisa Turashvili

Contents

G. Turashvili (✉)
Department of Pathology and Laboratory Medicine, Mount Sinai Hospital and University of Toronto, Toronto, ON, Canada
e-mail: Gulisa.Turashvili@sinaihealth.ca

R. A. Soslow et al. (eds.), *Atlas of Diagnostic Pathology of the Cervix*, https://doi.org/10.1007/978-3-030-49954-9_12

12.1 Melanocytic Tumors (Malignant Melanoma)

12.1.1 Definition

A malignant neoplasm composed of cells with melanocytic differentiation. The diagnosis of primary cervical malignant melanoma requires the demonstration of junctional activity in the epithelium in the absence of similar changes elsewhere in the body. The key features of malignant melanoma of the cervix are described in Table 12.1.

Table 12.1 Key features of cervical melanocytic tumors

Clinical presentation
• Asymptomatic
• Abnormal cervical cytology
• Abnormal bleeding
• Cervical mass
Macroscopy
• Single or multiple polypoid to fungating mass
• Pigmented mass
• Amelanotic mass
• Ulcerated mass
• Mean diameter 3 cm (range 0.3–9)
Microscopy
• Diffuse, nested, trabecular and/or fascicular growth patterns
• Tumor cells with epithelioid, spindled, round, or clear cytoplasm; large, vesicular to hyperchromatic nuclei; prominent nucleoli; brisk mitoses, including atypical forms
• Rarely multinucleated giant cells
• Variable intracytoplasmic melanin pigment, from abundant to absent
• Junctional activity in 50% of cases
• Pagetoid growth
• Stromal desmoplastic reaction
• Morris and Taylor criteria for primary gynecologic melanoma [18]:
1. Melanin in benign epithelium
2. Junctional activity
3. Absence of melanoma elsewhere
4. Metastases according to the pattern of gynecologic tumor
Immunohistochemistry
• Positive:
– S100 protein
– HMB-45
– Melan-A/MART-1
– MITF
– SOX10
• Negative:
– Cytokeratins
– Muscle markers (desmin, h-caldesmon, SMA)

HMB-45 human melanoma black 45, *Melan-A/MART-1* melanoma antigen recognized by T cells, *MITF* microphthalmia transcription factor, *SMA* smooth muscle actin, *SOX10* SRY-related HMG-box 10

12.1.2 Synonyms

Invasive melanoma.

12.1.3 Etiology

Primary cervical malignant melanoma has a melanocytic derivation. The proof of the presence of melanocytes in the cervical mucosa was first demonstrated in 3.5% of cervical biopsies in 1959 and further evidenced by diagnosing cervical melanocytic nevi [1–4]. Various hypotheses have been proposed for primary gynecologic melanomas, including its origin from Schwann cells, melanocyte migration from the neural crest, and melanocytic differentiation from the endocervical epithelium [2, 5–8]. No specific risk factors have been identified [9], but high levels of estrogen and association with human papillomavirus (HPV) infection and radiation therapy have been reported [10–12]. There are limited data on the distribution of mutations in primary cervical melanoma. However, non-vulvar gynecologic melanomas have been shown to harbor mutations in *KIT and NRAS* in approximately 30% of cases, while *BRAF* mutations are very rare.

12.1.4 Macroscopy

Malignant melanoma can present as single or multiple pigmented, polypoid to fungating masses or (in approximately 45% of cases) as amelanotic masses mimicking a primary cervical neoplasm [13, 14]. Ulceration may be present [15]. The mean diameter is 3 cm (range 0.3–9). Pigmented lesions are usually dark (blue, blue-black, blue-red, black, black-brown) or sometimes reddish (red, violet-red, brown-red, brown) [13].

12.1.5 Microscopy

Histologic features of primary cervical malignant melanoma are identical to cutaneous and mucosal melanoma. Diffuse, nested, trabecular, and/or fascicular growth patterns may be seen. Neoplastic cells exhibit epithelioid or spindled appearance, and rarely, round or clear cells. The nuclei are large, vesicular to hyperchromatic with prominent nucleoli and brisk mitotic activity, including atypical mitotic figures. Rarely multinucleated giant cells may be present. Melanin production can vary from abundant to focal or absent (Fig. 12.1). When present, melanin pigment granules are readily identified within the cytoplasm of tumor cells. In addition, approximately 50% of cases show junctional activity involving the overlying squamous epithelium. Pagetoid spread of tumor cells in the squamous epithelium may also be present. The tumor may invade the cervical mucosa with stromal desmoplastic reaction. Specific subtypes of primary cervical malignant melanoma, including a clear cell variant and a variant resembling a malignant peripheral nerve sheath tumor (MPNST), have been described [16, 17].

The four criteria proposed by Morris and Taylor for diagnosis of primary gynecological (vaginal) malignant melanoma include the presence of melanin in the benign epithelium, evidence of junctional activity, absence of melanoma elsewhere in the body, and the distribution of metastases that parallel the spread of squamous cell carcinoma [18]. These criteria may also be applied to cervical melanomas, but in many cases not all criteria are met; it can be difficult to establish definitively whether the melanoma is a primary or secondary lesion in the absence of cervical junctional changes. Clinical-pathologic correlation is essential in such cases.

Immunohistochemically, the tumor cells are positive for S100 protein, HMB-45 (human melanoma black 45), melan-A/MART-1 (melanoma antigen recognized by T cells), SOX10 (SRY-related HMG-box 10) and MITF (microphthalmia transcription factor); they are negative for cytokeratins and muscle markers. A combination of S100 (more sensitive) and HMB-45 (more specific) appears to lead to an accurate and reliable diagnosis in most cases [9, 13]. Ultrastructurally, the neoplastic cells contain intracytoplasmic pre-melanosomes and melanosomes.

Cytologic features range from small, round, deceptively bland cells to pleomorphic, bizarre-shaped cells. Smear preparations usually show single cells with central or eccentric nuclei with coarse chromatin and prominent nucleoli, irregular nuclear membranes, high nuclear-cytoplasmic ratio, and finely granular or wispy cytoplasm with intracytoplasmic melanin pigment. Nuclear molding, multinucleation, and intranuclear inclusions are common. The background shows tumor diathesis [13, 19].

Diagnostic Highlights

- Diffuse, nested, trabecular and/or fascicular growth patterns
- Tumor cells with epithelioid, spindled, round, or clear cytoplasm; large, vesicular to hyperchromatic nuclei; prominent nucleoli; brisk mitoses, including atypical forms
- Rarely multinucleated giant cells
- Variable intracytoplasmic melanin pigment, from abundant to absent
- Junctional activity in 50% of cases
- Pagetoid growth
- Stromal desmoplastic reaction
- Morris and Taylor criteria for primary gynecologic melanoma:
  1. Melanin in benign epithelium
  2. Junctional activity
  3. Absence of melanoma elsewhere
  4. Metastases according to the pattern of gynecologic tumor

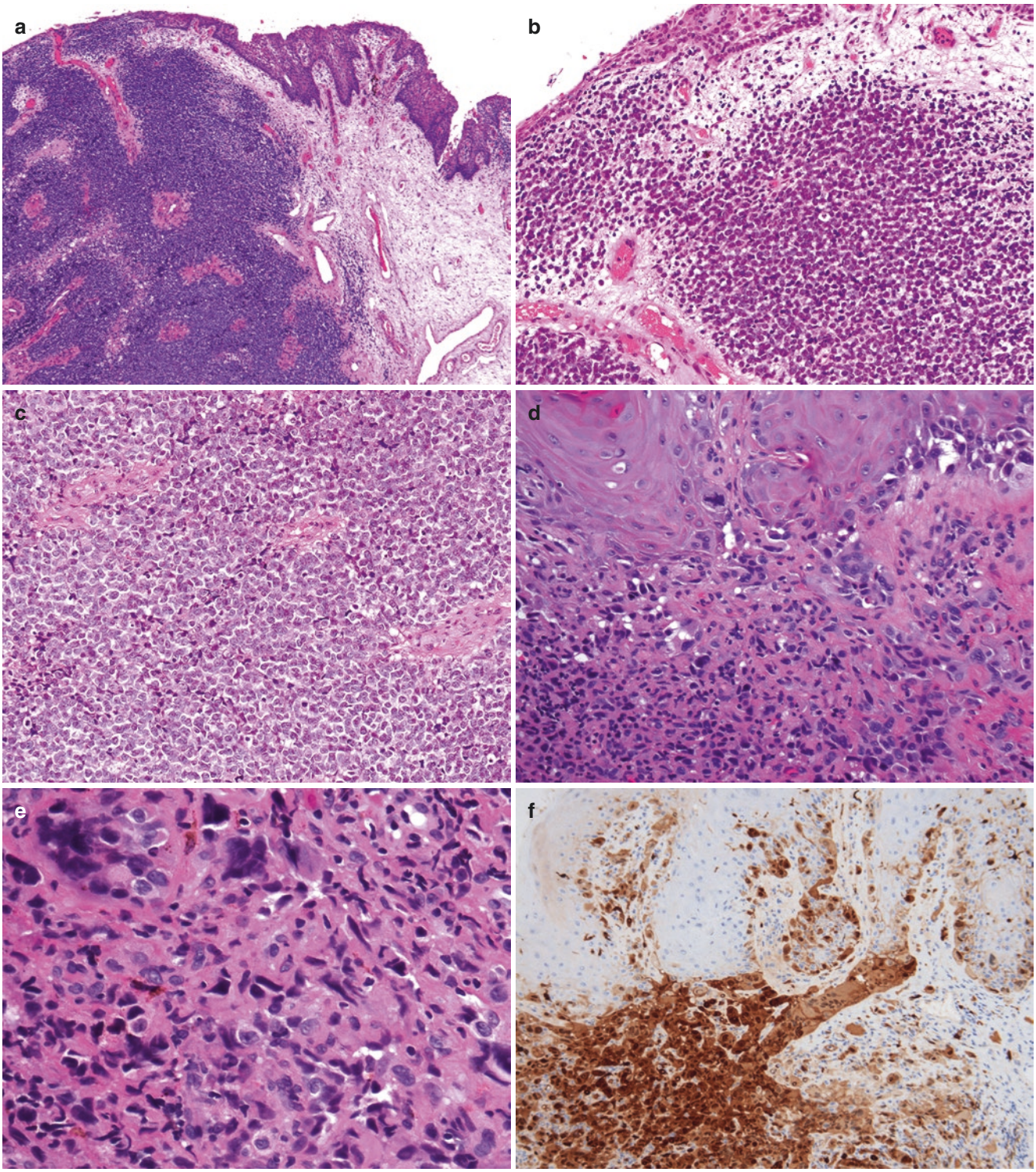

Fig. 12.1 Malignant melanoma. (**a–e**), Cervical biopsy with a nodular proliferation of high-grade neoplastic cells (H&E). There is epithelial ulceration (**a, b**). The tumor cells exhibit enlarged, irregular nuclei and prominent nucleoli (**c–e**). There is junctional activity in the squamous epithelium with atypical melanocytes and an atypical mitotic figure (**d**). Intracytoplasmic melanin pigment is present (**e**). (**f–h**), Immunohistochemical stains show diffuse, strong staining for S100 (**f**) and melan-A/MART-1 (**g**), and focal, moderate staining for HMB-45 (**h**). The patient has no prior history of cutaneous or mucosal malignant melanoma

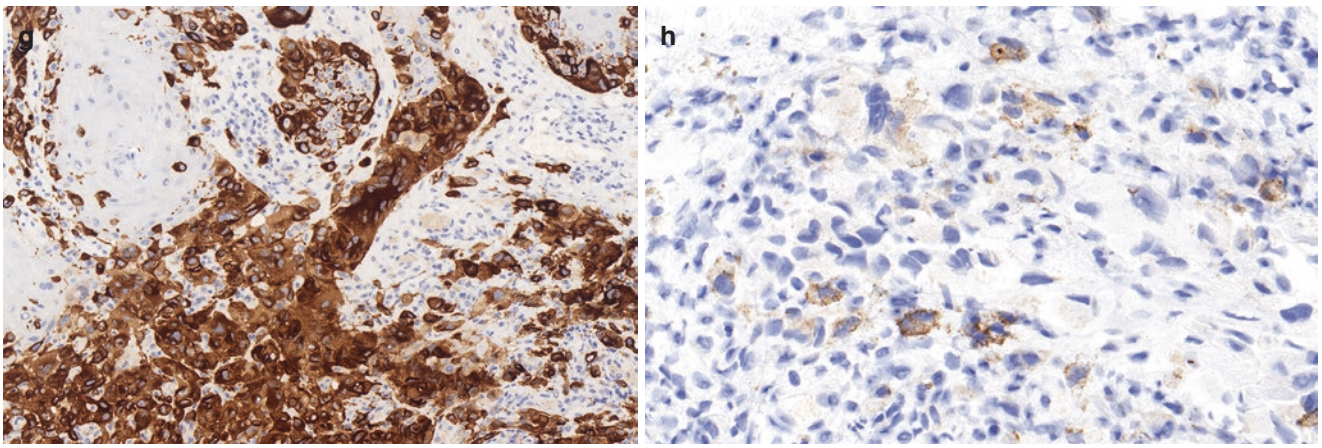

Fig. 12.1 (continued)

12.1.6 Differential Diagnosis

In the absence of melanin pigment, diagnosis of primary cervical malignant melanoma may be difficult [9, 20–23]. Table 12.2 outlines the main differential diagnostic considerations:

- *Poorly differentiated squamous cell carcinoma* shows at least focal keratin formation and/or intercellular bridges; may be associated with high-grade squamous intraepithelial lesion (HSIL); positive for high molecular weight keratin, p63, p40, and high-risk HPV subtypes; negative for melanocytic markers.
- *Poorly differentiated adenocarcinoma* shows at least focal gland formation or intracytoplasmic mucin; may be associated with adenocarcinoma in situ and HSIL; positive for low-molecular-weight keratin, CK7 (cytokeratin 7), and PAX8; negative for melanocytic markers. HPV-driven subtypes are also positive for high-risk HPV.
- *Leiomyosarcoma (epithelioid or spindle cell variants)* is comprised of diffuse sheets or intersecting fascicles of epithelioid or spindle cells; positive for muscle markers such as desmin, h-caldesmon, and SMA (smooth muscle actin); negative for melanocytic markers.
- *Embryonal rhabdomyosarcoma* shows a cellular subepithelial cambium layer with primitive cells with variable cytoplasmic cross-striations; positive for muscle markers; negative for melanocytic markers.
- *MPNST* shows densely cellular sweeping fascicles alternating with myxoid areas; rarely palisading, spindled to fusiform tumor cells with hyperchromatic and wavy nuclei, brisk mitoses, pale cytoplasm; necrosis, sometimes with melanin; variably positive for S100; negative for other melanocytic markers; may show loss of methylated H3K27.
- *High-grade endometrial stromal sarcoma* (*YWHAE type*) is comprised of high-grade round cells with nested or pseudoglandular patterns separated by thin-walled vessels; brisk mitoses; necrosis; variably positive, but usually negative for CD10, ER and PR (estrogen and progesterone receptors); negative for melanocytic markers.
- *Metastatic malignant melanoma* is characterized by absence of junctional activity; prior history of cutaneous or mucosal malignant melanoma elsewhere.

Table 12.2 Differential diagnosis of malignant melanoma of the cervix

	Clinical history	Microscopy	Ancillary studies	
			Positive	Negative
Primary malignant melanoma	No melanoma elsewhere, metastases according to the pattern of gynecologic tumor	Melanin in benign cervical epithelium; junctional activity; diffuse, nested, trabecular, and/or fascicular growth; tumor cells with epithelioid, spindled, round, or clear cytoplasm; large, vesicular to hyperchromatic nuclei; prominent nucleoli; brisk mitoses	S100, HMB-45, melan-A/MART-1, SOX10, MITF	Cytokeratins, desmin, h-caldesmon, SMA
Metastatic malignant melanoma	History of melanoma elsewhere	Similar to primary melanoma, lacks junctional activity	S100, HMB-45, melan-A/MART-1, SOX10, MITF	Cytokeratins, desmin, h-caldesmon, SMA
Cervical poorly differentiated squamous cell carcinoma	HSIL or invasive carcinoma	At least focal keratin formation and/or intercellular bridges	HMWK, p63, p40, high-risk HPV	S100, HMB-45, melan-A/MART-1, SOX10, MITF
Cervical poorly differentiated adenocarcinoma	AIS, HSIL or invasive adenocarcinoma	At least focal gland formation or intracytoplasmic mucin	LMWK, CK7, PAX8, high risk HPV in HPV-driven subtypes	S100, HMB-45, melan-A/MART-1, SOX10, MITF
Leiomyosarcoma, epithelioid or spindle cell	Sarcoma	Diffuse sheets or intersecting fascicles of epithelioid or spindle cells	Desmin, h-caldesmon, SMA, ±ER, PR, CD10, ±cytokeratins, EMA and HMB-45 in epithelioid subtype	S100 protein, melan-A/MART-1, SOX10, MITF
Rhabdomyosarcoma, embryonal	Sarcoma	Cellular subepithelial cambium layer, primitive cells, variable cytoplasmic cross striations	Desmin, MSA, myogenin (specific), myo-D1 (specific), myoglobin	S100, HMB-45, melan-A/MART-1, SOX10, MITF, SMA
Malignant peripheral nerve sheath tumor (MPNST)	Neurofibromatosis type 1, neurofibroma, MPNST elsewhere	Densely cellular sweeping fascicles alternating with myxoid areas; rarely palisading, spindled to fusiform tumor cells with hyperchromatic and wavy nuclei, pale cytoplasm, brisk mitoses; geographic necrosis, ±melanin	Variable S100 or SOX10 (not diffuse), cytokeratin in tumors mostly with glandular differentiation	HMB-45, melan-A/MART-1, MITF, methylated H3K27
High-grade endometrial stromal sarcoma (YWHAE type)	Uterine sarcoma	High-grade round cells with nested or pseudo-glandular patterns separated by thin-walled vessels; brisk mitoses; necrosis	BCOR, cyclin D1; variable CD10, ER, PR	S100, HMB-45, melan-A/MART-1, MITF, SOX10, desmin, h-caldesmon

AIS adenocarcinoma in situ, *CK7* cytokeratin 7, *EMA* epithelial membrane antigen, *ER* estrogen receptor, *HMWK* high molecular weight keratin, *HPV* human papillomavirus, *HSIL* high-grade squamous intraepithelial lesion, *HMB-45* human melanoma black 45, *LMWK* low molecular weight keratin, *MART-1* melanoma antigen recognized by T cells, *MITF* microphthalmia transcription factor, *MPNST* malignant peripheral nerve sheath tumor, *MSA* muscle specific actin, *PAX8* paired box 8, *PR* progesterone receptor, *SMA* smooth muscle actin, *SOX10* SRY-related HMG-box 10

12.1.7 Prognosis

Primary cervical malignant melanoma is usually diagnosed at an advanced stage and has an extremely unfavorable prognosis, similar to that of melanomas of other gynecologic (vaginal, vulvar) and non-gynecologic (anal, oronasal, esophageal) mucosal sites [9]. Patients with cervical malignant melanoma tend to develop local relapse rather than distant metastases. The most common sites are vagina, vulva, and suture line [13]. The most important prognostic factors are tumor stage and tumor thickness. Additional important features include lymphovascular space invasion (LVSI), the presence of lymphocytes, and neovascularization [9]. Mutation status has not been shown to have prognostic significance; however, patients with *KIT* (not uncommon) and *BRAF* (uncommon) mutations may be treated with targeted therapy.

Survival analysis of 78 cases showed that most patients (87.5%) died within 3 years of diagnosis, and 5-year survival was only 10.7%. The mean overall survival was 22.9 months and the median was 12 months (range 0.1–168). Furthermore, although 50% of patients were diagnosed at stage I, the 5-year survival rates were 18.8% for stage I, 11.1% for stage II, and 0% for stages III–IV. Treatment options include surgery alone and neoadjuvant, adjuvant, or palliative treatment with chemotherapy and/or radiation. Given the limited data, the optimal treatment strategy is unclear [9].

12.2 Germ Cell Tumors

12.2.1 Teratoma

12.2.1.1 Definition

Mature cystic teratoma is a tumor composed of mature tissues derived from more than one germ layer. The presence of immature tissue (typically neuroepithelium) defines an immature teratoma. The key features of mature and immature teratomas of the cervix are described in Table 12.3.

Table 12.3 Key features of cervical germ cell tumors

	Mature teratoma	Immature teratoma	Yolk sac tumor
Clinical presentation	Asymptomatic Abnormal cervical cytology Abnormal bleeding Cervical mass	Asymptomatic Abnormal cervical cytology Abnormal bleeding Cervical mass	Asymptomatic Abnormal cervical cytology Abnormal bleeding Cervical mass
Macroscopy	Cystic or solid lesions with hair and sebaceous material	Variable amount of solid areas	Polypoid mass Ulceration Friable, gray-white cut surface Hemorrhage and/or necrosis Mean size 5 cm (range 1–10)
Microscopy	Mature tissues of ectodermal, mesodermal, and endodermal derivation	Immature tissues, usually immature neuroepithelium Neuroepithelial tubules and rosettes lined by overlapping, hyperchromatic cells with brisk mitoses Cellular mitotically active glia Immature mesenchymal and endodermal elements (rare) Grading: a) 3-tiered: • 1 (immature elements in <1 LPF (40×) in any slide) • 2 (1–3 LPF in any slide) • 3 (>3 LPF in any slide) b) 2-tiered: • Low-grade /grade 1 • High-grade/grade 2–3	Multiple growth patterns including microcystic (most common), macrocystic, reticular, solid, papillary, polyvesicular vitelline Loose, myxoid to edematous stroma Schiller-Duval bodies in 50% Glandular or hepatoid differentiation (rare) Tumor cells with light eosinophilic to clear cytoplasm and primitive nuclei, often with prominent amphophilic nucleoli and brisk mitoses Intracytoplasmic hyaline bodies
Immunohistochemistry	Not required	*Positive:* GFAP, NSE, S100, SOX2, and glypican-3 in mature and immature neuroepithelium SALL4 in immature neuroepithelium, immature mesenchymal elements, mature and primitive enteric tissue OCT4 and PAX6 in immature neuroepithelium CD56 in mature neuroepithelium AFP in immature gastrointestinal-type glands or with hepatoid differentiation	*Positive:* SALL4 Glypican-3 AFP GATA3 LIN28 Variable CK7, EMA (usually focal), pan-cytokeratin, HNF1β, PAX8, CDX2, and TTF-1 Hep-Par1, albumin and CEA in hepatoid variant

AFP α-fetoprotein, *CK7* cytokeratin 7, *CDX2* caudal type homeobox 2, *CEA* carcinoembryonic antigen, *EMA* epithelial membrane antigen, *GATA3* GATA binding protein 3, *GFAP* glial fibrillary acidic protein, *Hep-Par1* hepatocyte paraffin 1, HNF1β hepatocyte nuclear 1β, *LPF* low power field, *NSE* neuron specific enolase, *OCT4* octamer-binding transcription factor 4, *PAX6* paired box 6, *PAX8* paired box 8, *SALL4* Sal-like protein 4, *TTF-1* thyroid transcription factor 1

12.2.1.2 Synonyms

Dermoid cyst.

12.2.1.3 Etiology

Four possible origins of uterine and cervical mature cystic teratomas include displaced germinal cells, pluripotential stem cells, metaplasia, and residual fetal tissue [24].

12.2.1.4 Macroscopy

Cystic or solid lesions containing sebaceous material and hair.

12.2.1.5 Microscopy

Mature cystic teratomas are composed of histologic structures of ectodermal, mesodermal, and endodermal derivation, most commonly skin and underlying cutaneous adnexal structures, as well as smooth and skeletal muscle and gastrointestinal or respiratory epithelium.

Immature teratomas exhibit variable amounts of immature tissues, typically neuroepithelial tubules and rosettes lined by overlapping, hyperchromatic cells with numerous mitotic figures and apoptotic bodies (Fig. 12.2). Cellular, mitotically active glia and immature cartilage, adipose tissue, bone, and skeletal muscle may be present. Immature endodermal structures (hepatic, renal, gastrointestinal) are less common. Based on the amount of immature neuroepithelial component, immature teratomas can be graded as grade 1 (immature elements in <1 low-power field [40×] in any slide), grade 2 (immature elements in 1–3 low-power fields in any slide), or grade 3 (immature elements in >3 low-power fields in any slide) [25], but a 2-tiered system is more commonly used (low-grade [grade 1] and high-grade [grades 2–3]) [26].

Immunohistochemically, GFAP (glial fibrillary acidic protein), NSE (neurospecific enolase), S100, SOX2, and glypican-3 are positive in both mature and immature neuroepithelium. SALL4 (Sal-like protein 4) is positive in immature neuroepithelium and mesenchymal elements, as well as mature and primitive enteric tissue. OCT4 (octamer-binding transcription factor 4) and PAX6 are positive in immature neuroepithelium, and CD56 is often positive in mature neuroepithelium. AFP (α-fetoprotein) may be positive in immature gastrointestinal-type glands.

Cytologic features in mature teratoma include fragments of benign epithelial cells (squamous, respiratory, gastrointestinal), sometimes with fragments of mesenchymal tissue (nerve, cartilage, adipose tissue) in a background of cystic contents. Immature teratoma shows malignant primitive-appearing cells.

Diagnostic Highlights

Mature cystic teratoma

- Mature tissues of ectodermal, mesodermal, and endodermal derivation

Immature teratoma

- Immature tissues, most obviously, immature neuroepithelium
- Neuroepithelial tubules and rosettes lined by overlapping, hyperchromatic cells with brisk mitoses
- Cellular glia that can be mitotically active
- Immature mesenchymal and endodermal elements (rare)
- 3-tiered grading:
  - 1 (immature elements in <1 LPF (40×) in any slide)
  - 2 (1–3 LPF in any slide)
  - 3 (>3 LPF in any slide)
- 2-tiered grading:
  - Low-grade / grade 1
  - High-grade / grade 2–3

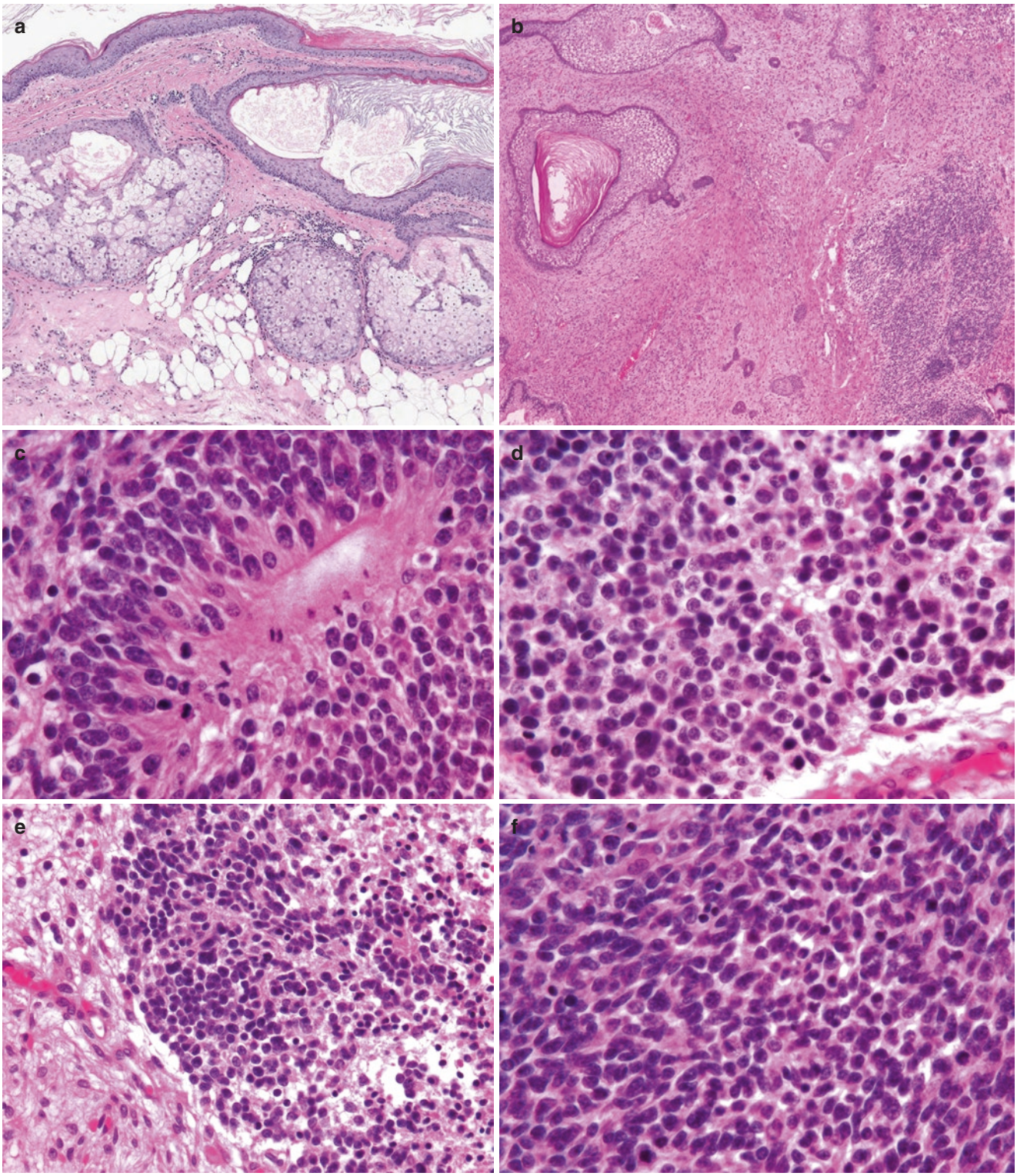

Fig. 12.2 Immature teratoma. (**a–f**), Total hysterectomy specimen with a low-grade immature teratoma (H&E). The tumor is composed predominantly of mature tissue elements such as skin and cutaneous appendages (**a, b**), cartilage, and small foci of immature neuroepithelium (**b–f**). The immature neuroepithelium is composed of tubules, rosettes and poorly defined clusters of overlapping, atypical, hyperchromatic cells with numerous mitotic figures and apoptotic bodies (**c–f**). The immature elements are seen in <1 low-power field (40×) in any slide. Therefore, the teratoma is graded as low-grade. The patient has no history of teratoma elsewhere

12.2.1.6 Differential Diagnosis

Mature cystic teratoma does not usually pose a diagnostic challenge. Table 12.4 outlines the main differential diagnostic considerations for immature teratoma:

- *Mature cystic teratoma with microscopic foci of neuroepithelium* shows mature teratomatous elements and microscopic foci of mature neuroepithelium lacking cytologic atypia or mitotic activity.
- *Malignant primitive neuroectodermal tumor.* The central type is composed of malignant cells closely resembling central nervous system neoplasms such as ependymoma, medulloblastoma, medulloepithelioma, neuroblastoma, ependymoblastoma, or glioblastoma multiforme. The peripheral type (akin to Ewing sarcoma) is composed of small, round, blue cells. Both are positive for CD99, FLI-1, CD56, S100, NSE, and rarely cytokeratin, and chromogranin. The central type is positive for GFAP, and the peripheral type shows *EWSR1* rearrangement, unlike the central type.
- *Carcinosarcoma* is usually diagnosed in older patients and shows high-grade epithelial and mesenchymal elements including malignant cartilage (as opposed to fetal cartilage), and, almost always, aberrant expression of p53.

Table 12.4 Differential diagnosis of germ cell tumors of the cervix

			Ancillary studies	
	Clinical history	Microscopy	Positive	Negative
Mature cystic teratoma with microscopic foci of neuroepithelium	Non-specific	Mature teratomatous elements and microscopic foci of mature neuroepithelium lacking cytologic atypia or mitoses	Not required	Not required
Carcinosarcoma	Older age and uterine corpus primary	High-grade epithelial and mesenchymal elements	Aberrant p53	SALL4, glypican-3, AFP
Malignant primitive neuroectodermal tumor	Non-specific	*Central type:* Malignant cells closely resembling CNS neoplasms such as ependymoma, medulloblastoma, medulloepithelioma, neuroblastoma, ependymoblastoma, glioblastoma multiforme *Peripheral type:* Small, round, blue cells, akin to Ewing sarcoma	*Both types:* CD99, FLI-1, CD56, S100, NSE, rare cytokeratin and chromogranin *Central type:* GFAP *Peripheral type: EWSR1* rearrangement	SALL4, glypican-3, AFP
Yolk sac tumor	Non-specific	Multiple growth patterns (microcystic, macrocystic, reticular, solid, papillary, and polyvesicular vitelline); Schiller-Duval bodies in 50%; rarely glandular or hepatoid differentiation; tumor cells with eosinophilic to clear cytoplasm and primitive nuclei, prominent nucleoli, and brisk mitoses; intracytoplasmic hyaline bodies	SALL4, glypican-3, AFP, GATA3, LIN28, Variable HNF1β, pan-cytokeratin, PAX8, CDX2, TTF-1; CK7, EMA (usually focal); CEA, Hep-Par1 and albumin in hepatoid variant	Wild-type p53
Mixed tumor or spindle cell epithelioma	Reproductive-age women	Well-circumscribed, biphasic lesion with spindle cells and focal squamous or glandular component; bland cytology	Variable EMA, ER, PR, muscle markers	SALL4, glypican-3, AFP, TTF-1
Clear cell adenocarcinoma	Bimodal (young and perior postmenopausal women with or without DES exposure)	Tubulocystic, solid and/or papillary growth patterns	PAX8, EMA, CK7, napsin-A, racemase, HNF1β	SALL4, glypican-3, AFP, TTF-1, ER, PR
Rhabdomyosarcoma, embryonal	Sarcoma	Cellular subepithelial cambium layer, primitive cells with cytoplasmic cross striations (variable)	Desmin, MSA, myogenin, myo-D1, myoglobin, variable SMA	SALL4, glypican-3, AFP
Mesonephric adenocarcinoma	Adult women	Glomeruloid, tubular, papillary or solid growth	GATA3 and/or TTF-1, PAX8	ER, PR

AFP α-fetoprotein, *CDX2* caudal type homeobox 2, *CEA* carcinoembryonic antigen, *CK7* cytokeratin 7, *CNS* central nervous system, *DES* diethylstilbestrol, *EMA* epithelial membrane antigen, *ER* estrogen receptor, *FLI-1* friend leukemia integration 1, *GATA3* GATA binding protein 3, *GFAP* glial fibrillary acidic protein, *Hep-Par1* hepatocyte paraffin 1, *HNF1β* hepatocyte nuclear 1β, *MSA* muscle-specific actin, *NSE* neuron specific enolase, *PAX8* paired box 8, *PR* progesterone receptor, *SALL4* Sal-like protein 4, *SMA* smooth muscle actin, *TTF-1* thyroid transcription factor 1

12.2.1.7 Prognosis

Both mature and immature cystic teratomas of the cervix have had a benign clinical course in all case reports published to date [27–30].

12.2.2 Yolk Sac Tumor

12.2.2.1 Definition

A primitive malignant germ cell tumor with various histologic patterns recapitulating developmental phases of the normal yolk sac. Rarely, yolk sac tumors may also arise from epithelial neoplasms of gynecologic origin such as endometrioid, high-grade serous or clear cell adenocarcinoma. These somatically derived yolk sac tumors typically occur in older patients and have overlapping morphology and immunophenotype with the epithelial neoplasm; they are not the topic of this discussion. The key features of yolk sac tumor of the cervix are described in Table 12.3.

12.2.2.2 Synonyms

Endodermal sinus tumor.

12.2.2.3 Etiology

The most likely cause is aberrant migration of primordial germ cells. The tumor typically affects the vagina or cervix in young children aged less than 4 years [31, 32], and it can be challenging to establish the primary site [33, 34].

12.2.2.4 Macroscopy

Typically, polypoid mass, frequently ulcerated, with a friable, gray to white cut surface with areas of hemorrhage and/or necrosis. The mean tumor size is 5 cm (range 1–10).

12.2.2.5 Microscopy

The histologic features are identical to those of ovarian and vaginal yolk sac tumors and include a variety of growth patterns such as reticular, microcystic, solid, papillary, and polyvesicular vitelline, with the microcystic pattern being the most common [31, 33]. The stroma may be loose, myxoid to edematous. Approximately 50% of cases show pathognomonic Schiller-Duval bodies comprising papillary structures with a central vascular channel covered by cuboidal to columnar cells, separated by an acellular zone of connective tissue. Schiller-Duval bodies may be difficult to find and may be present only focally. Glandular or hepatoid differentiation may be seen. The tumor cells exhibit variable amounts of light eosinophilic to clear cytoplasm and primitive nuclei, often with prominent amphophilic nucleoli and frequent mitotic figures. Intracytoplasmic hyaline bodies may be present (Fig. 12.3).

Immunohistochemically, the tumor cells are positive for SALL4, glypican-3, AFP, GATA3, and LIN28 [35, 36]. Pancytokeratin, HNF1β, PAX8, CDX2, and TTF-1 (thyroid transcription factor 1) may be positive. CK7 and EMA (epithelial membrane antigen) are only focally expressed in a minority of tumors. The hepatoid variant is usually positive for CEA (carcinoembryonic antigen), Hep-Par1 (Hepatocyte Paraffin 1) and albumin.

Cytologic features include sheets of malignant cells with irregular nuclear contours, coarse chromatin, and vacuolated cytoplasm. Schiller-Duval bodies (glomerular-like structures) and hyaline globules may be present. The background contains metachromatic basement membrane–like material.

Diagnostic Highlights

- Multiple growth patterns including microcystic (most common), macrocystic, reticular, solid, papillary, polyvesicular vitelline
- Loose, myxoid to edematous stroma
- Schiller-Duval bodies in 50%
- Glandular or hepatoid differentiation (rare)
- Tumor cells with light eosinophilic to clear cytoplasm and primitive nuclei, often with prominent amphophilic nucleoli and brisk mitoses
- Intracytoplasmic hyaline bodies

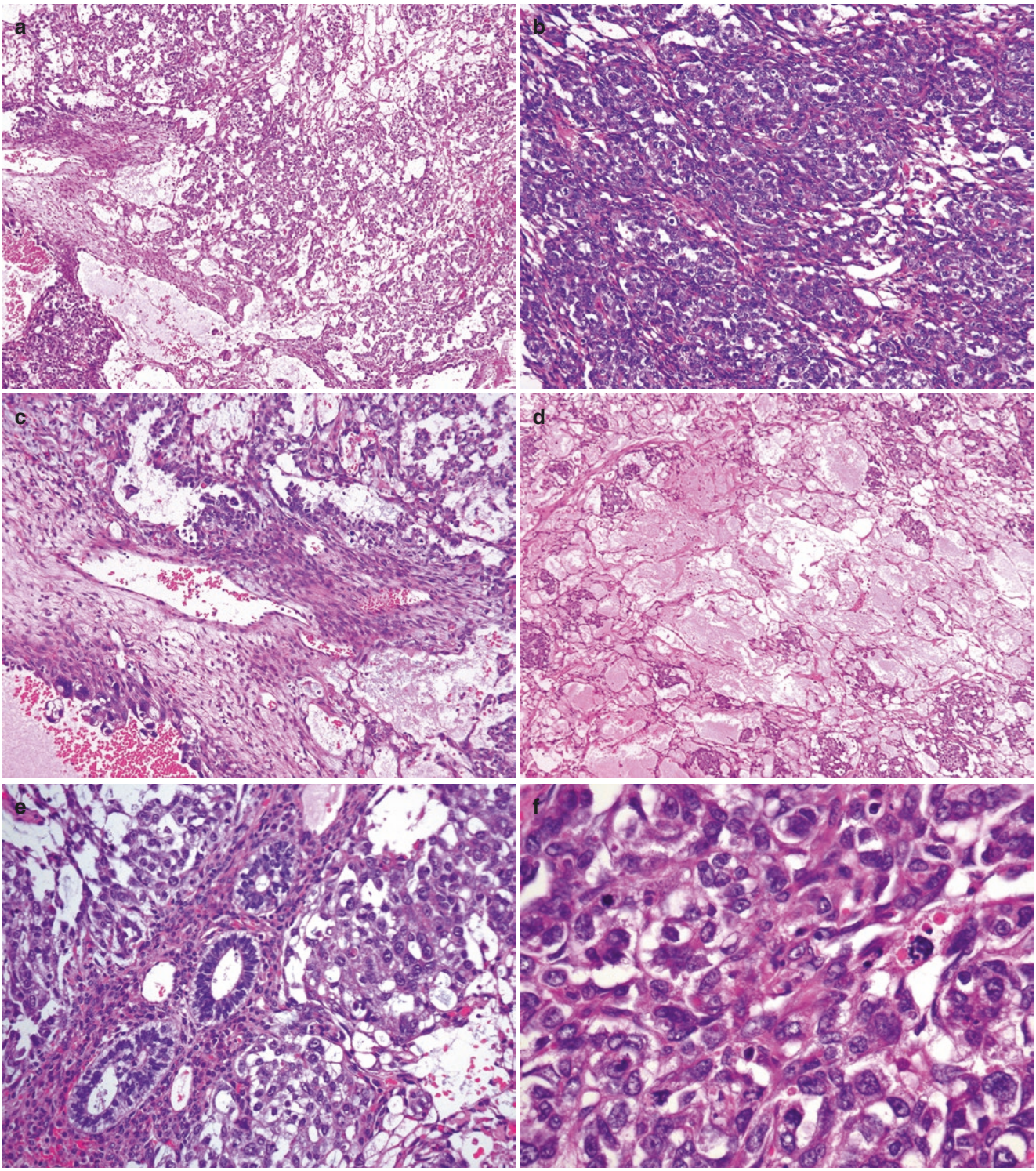

Fig. 12.3 Yolk sac tumor. (**a–h**), Total hysterectomy specimen with a primitive-appearing neoplasm (H&E). Various growth patterns include microcystic or macrocystic (**a**), solid (**b**), glandular (**c**), polyvesicular vitelline with numerous small vesicles surrounded by connective tissue (**d**) and endoderm resembling secretory endometrium (**e**). The tumor cells exhibit high-grade nuclei with numerous mitotic figures (**f**), hyaline globules (**g**), and Schiller-Duval bodies (**h**). **i–l**, Immunohistochemical stains show strong, diffuse staining for SALL4 (**i**) and pan-cytokeratin (**j**), with patchy staining for GATA3 (**k**) and focal staining for CK7 (**l**)

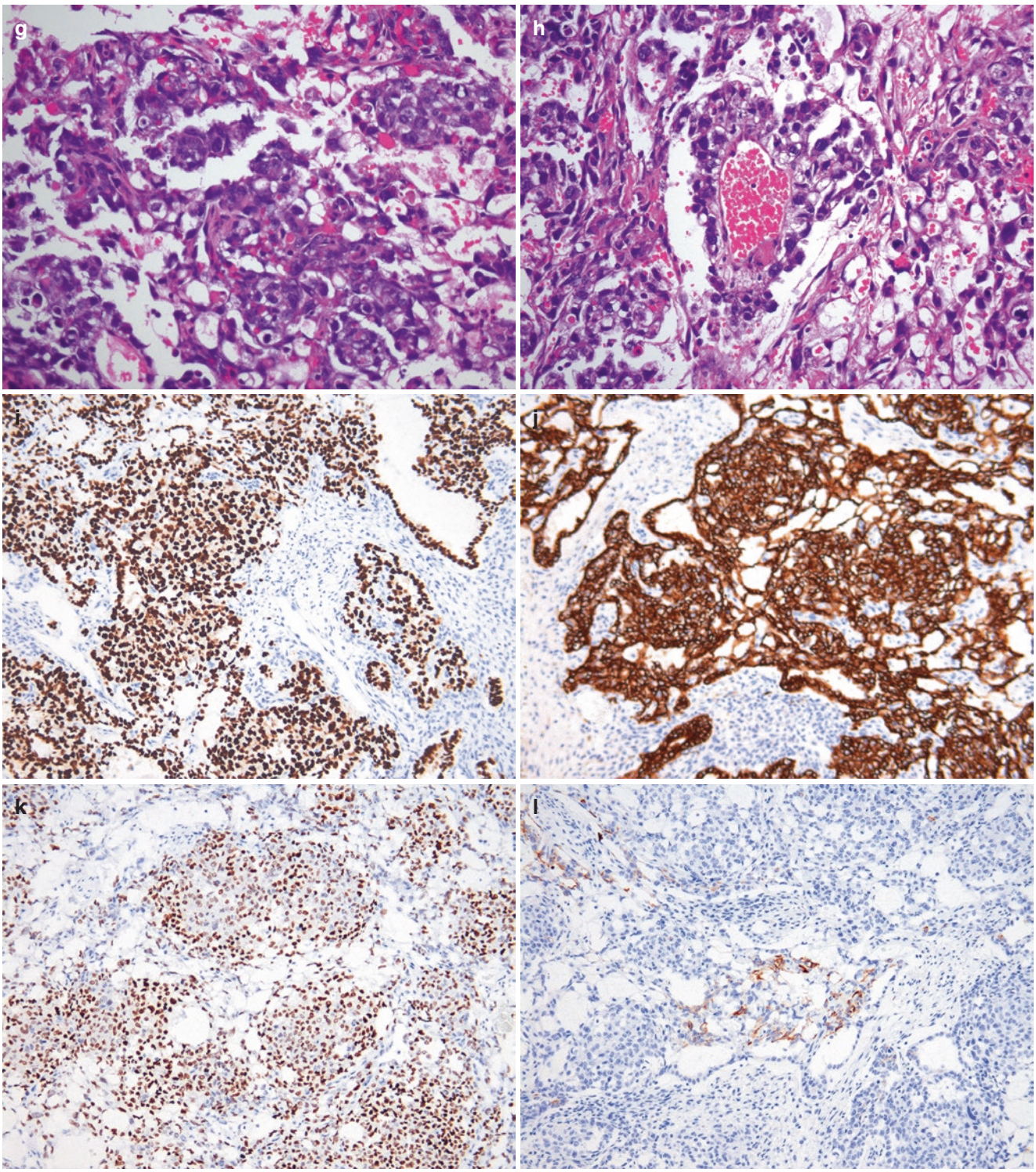

Fig. 12.3 (continued)

12.2.2.6 Differential Diagnosis

Table 12.4 outlines the top differential diagnoses:

- *Mixed tumor or spindle cell epithelioma* is usually diagnosed in women of reproductive age; a well-circumscribed biphasic lesion composed of fascicular spindle cells and focal squamous or glandular epithelial cells with bland cytology, eosinophilic hyaline globules; variable positivity for keratin, ER, PR, and muscle markers.
- *Clear cell adenocarcinoma* typically affects young and perimenopausal or postmenopausal women with or without diethylstilbestrol exposure and shows tubulocystic, solid, and/or papillary growth patterns; positive for PAX8, EMA, CK7, napsin-A, racemase and HNF1β (hepatocyte nuclear 1β); typically negative for ER and PR.
- *Embryonal rhabdomyosarcoma* shows a cellular subepithelial cambium layer and primitive cells with variable presence of cytoplasmic cross-striations; positive for desmin, MSA (muscle specific actin), myoglobin, myogenin, and myo-D1. The latter two markers are specific for skeletal muscle differentiation.
- *Mesonephric adenocarcinoma* affects adult women, and shows "endometrioid-like morphology" frequently admixed with glomeruloid, papillary, tubular or solid growth patterns and, occasionally a background of mesonephric hyperplasia; positive for PAX8, GATA3, and/or TTF-1; negative for ER and PR.

The prognosis for patients with cervicovaginal yolk sac tumors is favorable with platinum-based chemotherapy; cure rates are >95% [37–39]. Serum AFP levels are useful for monitoring therapy and for followup. Recurrence typically occurs within 2 years of treatment and carries a poor prognosis [38].

12.2.3 Choriocarcinoma

Pure non-gestational choriocarcinoma is considered a primary germ cell neoplasm. Primary cervical non-gestational choriocarcinoma is extremely rare [40, 41] and displays morphologic and immunohistochemical features similar to those of gestational choriocarcinoma, as discussed in Sect. 12.3 below.

12.3 Trophoblastic Tumors

12.3.1 Choriocarcinoma

12.3.1.1 Definition

Choriocarcinoma can be divided into gestational and non-gestational subtypes. Gestational choriocarcinoma is a malignant trophoblastic tumor consisting of a trimorphic proliferation of intermediate trophoblastic cells, syncytiotrophoblast and cytotrophoblast, in the absence of chorionic villi. Pure non-gestational choriocarcinoma is a germ cell neoplasm. In addition, choriocarcinomatous differentiation may occur in a variety of poorly differentiated somatic neoplasms of gynecologic or non-gynecologic origin [42, 43]. Thus, a malignant tumor with trophoblastic differentiation involving the uterine cervix may be a gestational or non-gestational choriocarcinoma and may represent a primary tumor or a metastasis from other organs. The key features of gestational choriocarcinoma are described in Table 12.5.

Table 12.5 Key features of cervical trophoblastic tumors

	Placental site trophoblastic tumor	Epithelioid trophoblastic tumor	Choriocarcinoma
Clinical presentation	Mean age 30–32 years (range 20–63) Vaginal bleeding or amenorrhea 2 weeks to 17 years from last pregnancy May follow normal pregnancy (most) or spontaneous abortion (16%)	Mean age 36 years (range 15–48) Vaginal bleeding or amenorrhea 1–25 years from last pregnancy May follow normal term pregnancy (67%), molar pregnancy (16%), or spontaneous abortion (16%) Possible precursor: Atypical placental site nodule	Mean age 29–31 years (range 15–48) Vaginal bleeding A few months to 14 years from last pregnancy May follow molar pregnancy (50%), spontaneous abortion (25%), or normal term pregnancy (25%)
Macroscopy	Expansile endophytic or exophytic mass Infiltrative, poorly circumscribed solid mass Size 1–10 cm Solid and fleshy, white-tan to light yellow cut surface with focal hemorrhage and necrosis Mass may extend to serosa, broad ligament, or adnexa Much more common in uterine corpus	Expansile endophytic or exophytic mass with pushing borders Size 0.5–5 cm Solid or cystic Hemorrhage and necrosis More common in uterine cervix and lower uterine segment	Single or multiple bulky and destructive, dark red masses Infiltrative or circumscribed Hemorrhage and necrosis Destructive growth in surrounding tissues More common in uterine corpus
Cell of origin	Implantation site intermediate trophoblast	Chorionic-type intermediate trophoblast	Villous intermediate trophoblast, syncytiotrophoblast, and cytotrophoblast

Table 12.5 (continued)

	Placental site trophoblastic tumor	Epithelioid trophoblastic tumor	Choriocarcinoma
Microscopy	Central sheets and peripheral cords and nests of intermediate trophoblast cells Round to polygonal tumor cells with eosinophilic to clear cytoplasm and moderate to marked cytologic atypia Mitoses up to 6 per 10 high-power fields Rare multinucleated cells resembling syncytiotrophoblast Infiltrative borders with tumor cells separating myometrial smooth muscle fibers at tumor periphery Large nests of tumor cells replacing vascular walls Associated eosinophilic extracellular matrix Necrosis may be present	Sheets, nests, and cords of intermediate trophoblast cells Rare syncytiotrophoblast Central small vessel Hyaline-like material May colonize cervical mucosal epithelium Mild to moderate cytologic atypia with prominent nucleoli Mitoses up to 9 per 10 high-power fields Decidualized stromal cells at tumor periphery Necrosis	Trimorphic pattern with three types of trophoblast (villous intermediate trophoblast, syncytiotrophoblast, cytotrophoblast) Marked cytologic atypia Mitoses up to 22 per 10 high-power fields Extensive hemorrhage and necrosis No chorionic villi LVSI
Immunohistochemistry	*Positive:* Diffusely positive for hPL, Mel-CAM, HSD3B1, CD10, pan-cytokeratin, CK18, EMA, GATA3, MUC4, HLA-G Focally positive for PLAP Positive β-hCG and inhibin-α in scattered multinucleated cells Ki-67 10–30% *Negative:* p63 SALL4	*Positive:* Diffusely positive for p63, PLAP, pan-cytokeratin, CK18, EMA, inhibin-α, HLA-G, GATA3, H3D3B1, cyclin E, CD10, inhibin-α Variable hPL, Mel-CAM, β-hCG Ki-67 10–25% *Negative:* SALL4	*Positive:* β-hCG diffusely positive in syncytiotrophoblast, weakly and focally positive in cytotrophoblast or intermediate trophoblast Diffuse HSD3B1 in syncytiotrophoblast Mel-CAM, HLA-G, and MUC4 in intermediate trophoblast Diffuse keratin Variable hPL, SALL4, p63, inhibin-α Ki-67 > 90%

β-hCG β human chorionic gonadotropin, *CK18* cytokeratin 18, *EMA* epithelial membrane antigen, *GATA3* GATA binding protein 3, *HLA-G* human leukocyte antigen G, *hPL* human placental lactogen, *LVSI* lymphovascular space invasion, *Mel-CAM* melanoma cell adhesion molecule, *MUC4* mucin 4, *PLAP* placental alkaline phosphatase, *SALL4* Sal-like protein 4

12.3.1.2 Synonyms

Chorioepithelioma, chorionepithelioma.

12.3.1.3 Etiology

Gestational choriocarcinoma may arise due to progression of a complete or partial hydatidiform mole, or it may arise after a normal term pregnancy or an ectopic pregnancy [44, 45], with 50% of gestational choriocarcinomas occurring after complete hydatidiform mole, 25% after spontaneous abortion, and 25% after normal term pregnancy. The risk of developing choriocarcinoma is approximately 2% to 3% following a complete mole and 0.1% to 0.5% following a partial mole [46]. Non-gestational choriocarcinoma is likely to have the same origin as the other germ-cell tumors discussed above.

12.3.1.4 Macroscopy

Single or multiple bulky and destructive dark red masses with hemorrhage and necrosis.

12.3.1.5 Microscopy

Choriocarcinoma may be circumscribed but usually shows invasive and destructive growth in surrounding tissues. There is a trimorphic pattern consisting of all three types of trophoblast: large intermediate trophoblast with abundant amphophilic to eosinophilic cytoplasm, smaller cytotrophoblast, and multinucleated syncytiotrophoblast. There is conspicuous mitotic activity, up to 22 per 10 high-power fields. Extensive recent and remote hemorrhage and necrosis are seen (Fig. 12.4). LVSI is common. No residual chorionic villi are present.

Immunohistochemically, β-hCG (β human chorionic gonadotropin) and HSD3B1 show diffuse staining in syncytiotrophoblast, with weak and focal expression of β-hCG in the cytotrophoblast or intermediate trophoblast cells. The intermediate trophoblast cells are positive for Mel-CAM/CD146 (melanoma cell adhesion molecule), HLA-G (human leukocyte antigen G) and MUC4 (mucin 4). Keratin is diffusely positive, and hPL (human placental lactogen), SALL4, p63 and inhibin-α show variable staining. The Ki-67 labeling index is usually >90%.

Cytologic features include clusters of syncytiotrophoblast and cytotrophoblast in a background of tumor diathesis.

Diagnostic Highlights

- Trimorphic pattern with three types of trophoblast (villous intermediate trophoblast, syncytiotrophoblast, cytotrophoblast)
- Marked cytologic atypia
- Mitoses up to 22 per 10 high-power fields
- Extensive hemorrhage and necrosis
- No chorionic villi
- LVSI

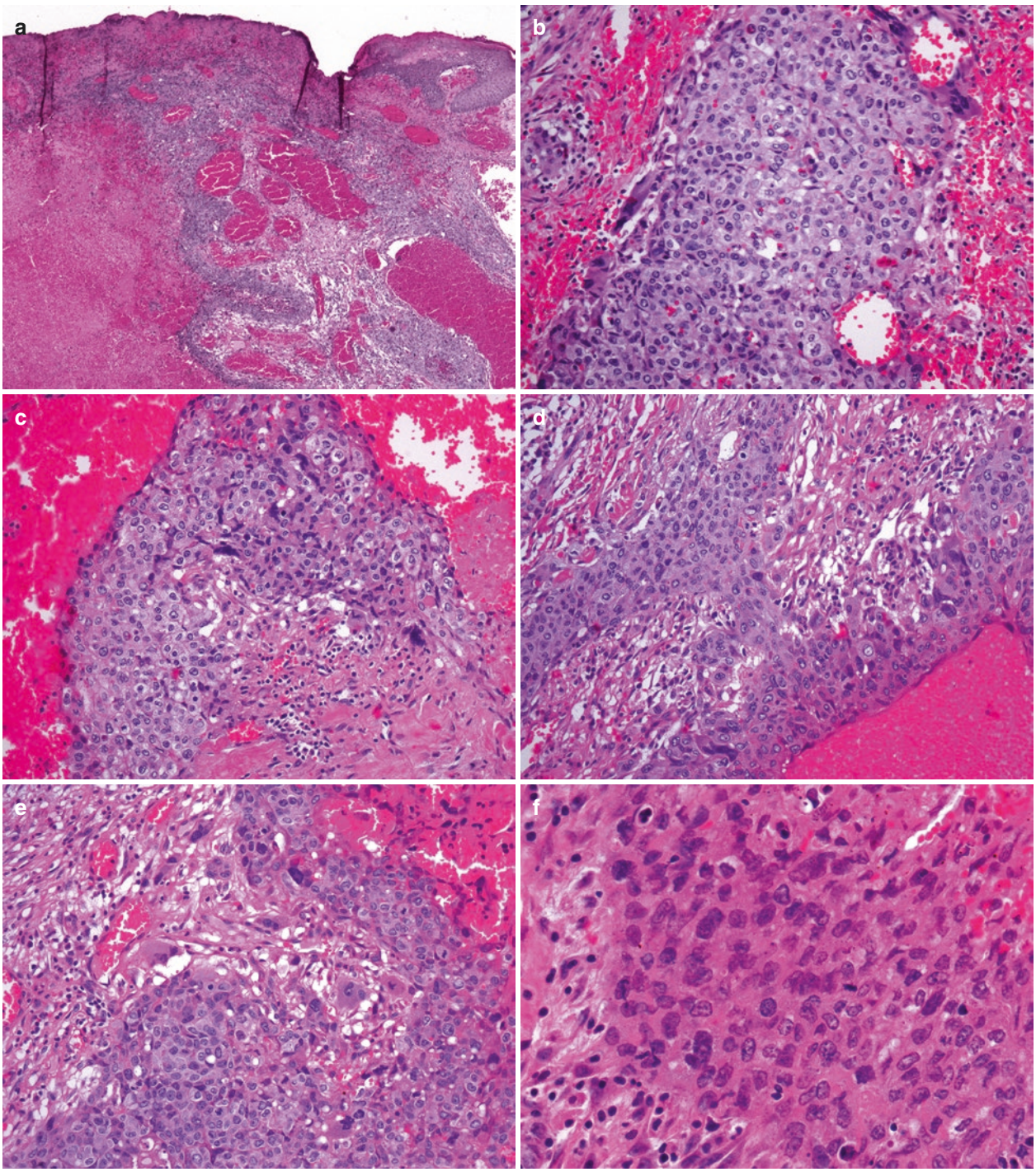

Fig. 12.4 Gestational choriocarcinoma. (**a–h**), Total hysterectomy specimen with a markedly atypical mass-forming lesion containing multiple foci of necrosis and hemorrhage and ulceration of the overlying squamous epithelium (H&E). The tumor is composed predominantly of medium-sized cytotrophoblast and intermediate trophoblast and scattered large, multinucleated syncytiotrophoblast cells (**b–h**). Chorionic villi are not present. (**i**) An immunohistochemical stain for β-hCG shows strong, diffuse staining in both the syncytiotrophoblast (the most darkly stained cells) and cytotrophoblast cells

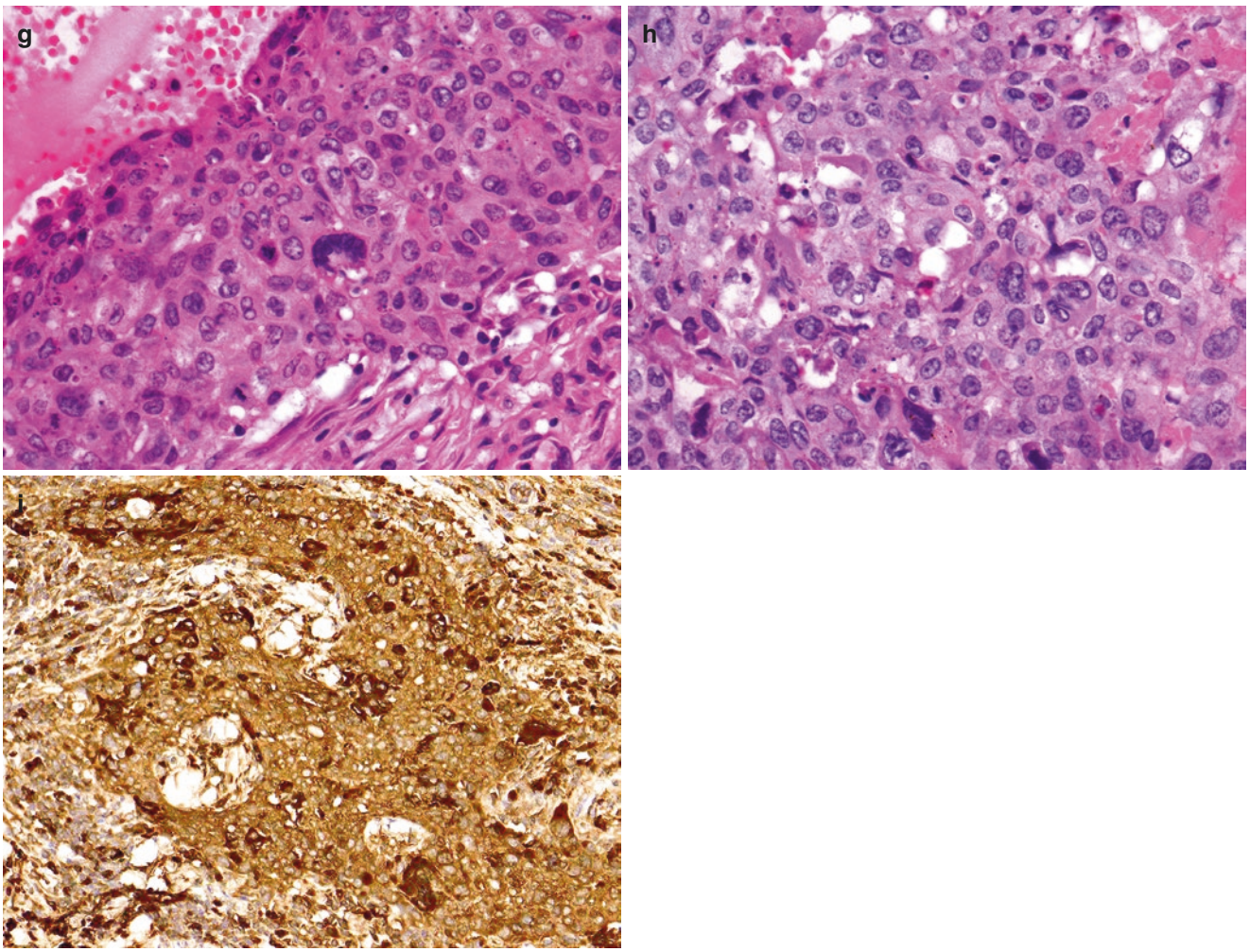

Fig. 12.4 (continued)

12.3.1.6 Differential Diagnosis

Table 12.6 outlines the top differential diagnoses for trophoblastic tumors involving the cervix:

- *Epithelioid trophoblastic tumor* is well-circumscribed; composed predominantly of nests or cords of chorionic-type intermediate trophoblast with only rare syncytiotrophoblast; eosinophilic fibrinoid matrix; no diffuse β-hCG.
- *Placental site trophoblastic tumor* is usually an infiltrating mass; composed of confluent sheets or infiltrating monomorphic implantation-site intermediate trophoblast; variable necrosis; no diffuse β-hCG.
- *Non-gestational choriocarcinoma* shows identical profiles to the patient's benign tissue by DNA polymorphism analysis or short tandem repeat genotyping [47, 48].
- *Invasive mole* shows residual hydropic chorionic villi; loss of p57 staining in cytotrophoblast and villous stromal cells in complete mole.
- *Normal immature trophoblast of early gestation in curettings* lacks significant cytologic atypia, necrosis, or destructive growth; found in small quantities; chorionic villi may be seen on deeper sectioning.
- *Exaggerated placental site* is usually an incidental microscopic finding composed of implantation-site trophoblastic cells separated by hyalinized stroma and lacking mitotic activity; admixed with chorionic villi and fragments of decidua; absence of confluent masses (Fig. 12.5). Frequently associated with molar pregnancies.
- *Poorly differentiated carcinoma with trophoblastic differentiation* may show areas of more conventional carcinoma.
- *Poorly differentiated carcinoma with anaplastic features or giant cells* lacks admixture of cytotrophoblast and syncytiotrophoblast; positive for EMA; negative or weakly positive for β-hCG.

Table 12.6 Differential diagnosis of trophoblastic tumors involving the cervix

	Clinical history	Microscopy	Ancillary studies	
			Positive	Negative
Epithelioid trophoblastic tumor	Term pregnancy, complete or partial mole, spontaneous abortion, previous diagnosis of atypical placental site nodule, vaginal bleeding or amenorrhea	Well circumscribed, composed of nests or cords of chorionic-type intermediate trophoblast with rare syncytiotrophoblast, eosinophilic fibrinoid matrix	Diffuse p63, PLAP, cytokeratin, EMA, inhibin-α, GATA3, H3D3B1, HLA-G, cyclin E, inhibin-α Focal hPL, Mel-CAM, β-hCG Ki-67 10–25%	SALL4
Placental site trophoblastic tumor	Term pregnancy, spontaneous abortion, vaginal bleeding, or amenorrhea	Infiltrating, composed of confluent sheets or infiltrating monomorphic implantation-site intermediate trophoblast; less extensive to no necrosis	Diffuse hPL, Mel-CAM, cytokeratin, EMA, GATA3, MUC4, HSD3B1, HLA-G Focal PLAP β-hCG and inhibin-α in scattered multinucleated cells Ki-67 10–30%	p63, SALL4
Choriocarcinoma, gestational	Complete or partial hydatidiform mole, spontaneous abortion, or normal term pregnancy, vaginal bleeding	Biphasic tumor with three constituents: cytotrophoblast and intermediate trophoblast surrounded by syncytiotrophoblast, with extensive necrosis and hemorrhage; DNA polymorphism analysis or STR genotyping showing different profiles between the tumor and patient's benign tissue	β-hCG diffuse in syncytiotrophoblast, weak and focal in cytotrophoblast or intermediate trophoblast Diffuse hPL and HSD3B1 in syncytiotrophoblast Variable hPL, SALL4, p63, inhibin-α Ki-67 > 90%	p16
Choriocarcinoma, non-gestational	Ovarian germ cell tumor	Morphology similar to gestational choriocarcinoma, but DNA polymorphism analysis or STR genotyping shows identical profiles between the tumor and patient's benign tissue	β-hCG diffuse in syncytiotrophoblast, weak and focal in cytotrophoblast or intermediate trophoblast Diffuse hPL and HSD3B1 in syncytiotrophoblast Variable hPL, SALL4, p63, inhibin-α Ki-67 > 90%	p16
Invasive mole	Complete or partial hydatidiform mole	Residual chorionic villi; trophoblastic proliferation in complete mole may predominate over villi	Retained p57 in cytotrophoblast and villous stromal cells in partial mole	Loss of p57 in cytotrophoblast and villous stromal cells in complete mole
Poorly differentiated carcinoma with trophoblastic differentiation	Cervical cancer	Areas of more conventional carcinoma present, no paternal genome by STR genotyping	β-hCG	PAX8, p63
Poorly differentiated carcinoma with anaplastic features or giant cells	Cervical cancer	Lacks admixture of cytotrophoblast and syncytiotrophoblast, no paternal genome by STR genotyping	EMA, diffuse p16 if associated with high-risk HPV, aberrant p53	β-hCG, PAX8, p63
Normal immature trophoblast of early gestation in curettings	None	No significant cytologic atypia, necrosis, or destructive growth, small quantities, chorionic villi on deeper sectioning	p63	β-hCG

Table 12.6 (continued)

	Clinical history	Microscopy	Ancillary studies	
			Positive	Negative
Exaggerated placental site	Incidental, often found with molar pregnancies	Implantation-site trophoblastic cells separated by hyalinized stroma and lacking mitotic activity, admixed with chorionic villi and fragments of decidua; absence of confluent masses	CK18	β-hCG, p63
Placental site nodule	Incidental	Single or multiple well-circumscribed oval nodules or plaques, <5 mm in size Chorionic-type intermediate trophoblast cells arranged singly or in cords within hyalinized matrix; no cytologic atypia or mitotic activity; the center of nodules may be less cellular	PLAP, p63, CD10, cytokeratin, EMA Focal hPL, Mel-CAM, inhibin-α Rarely, β-hCG Ki-67 < 8%	β-hCG
Atypical placental site nodule	Incidental	Nodules measuring 5–10 mm, more cellular with cytologic atypia and some mitotic activity	PLAP, p63, CD10, cytokeratin, EMA Focal hPL, Mel-CAM, inhibin-α Rarely β-hCG Ki-67 8–10%	β-hCG
Squamous cell carcinoma	HSIL or carcinoma	At least focal keratinization or intercellular bridges; lacking decidualized benign stromal cells at tumor periphery	p63, p40, HMWK, diffuse p16, high-risk HPV	Inhibin-α, HLA-G, Mel-CAM, hPL, CK18 (most cases)
Epithelioid leiomyosarcoma	Sarcoma	Sheets and fascicles of epithelioid cells with marked atypia and mitoses	Desmin, h-caldesmon, SMA, ±ER, PR, EMA, cytokeratin	p63, hPL, β-hCG

β-hCG β human chorionic gonadotropin, *CK18* cytokeratin 18, *EMA* epithelial membrane antigen, *ER* estrogen receptor, *GATA3* GATA binding protein 3, *HLA-G* human leukocyte antigen G, *hPL* human placental lactogen, *HMWK* high-molecular-weight keratin, *HSIL* high-grade squamous intraepithelial lesion, *Mel-CAM* melanoma cell adhesion molecule, *MUC4* mucin 4, *PAX8* paired box 8, *PLAP* placental alkaline phosphatase, *PR* progesterone receptor, *SALL4* Sal-like protein 4, *SMA* smooth muscle actin, *STR* short tandem repeat

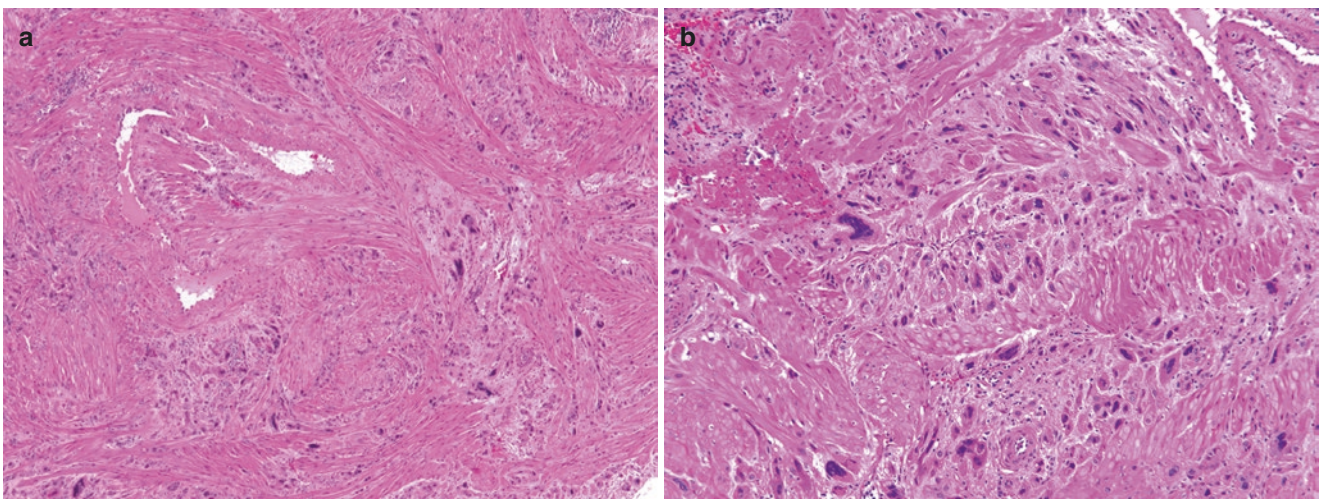

Fig. 12.5 Exaggerated placental site. (**a–d**), Endocervical curettings for retained products of conception (H&E). There are fragments of endomyometrium with an increased number of mononucleated and multinucleated implantation-site intermediate trophoblast cells with abundant eosinophilic cytoplasm, with hyperchromatic and irregular nuclei. The cells are widely spaced and lack mitotic activity. There is no necrosis (**a–d**). Scant chorionic villi are also present (**d**). (**e** and **f**), Immunohistochemical stains show the trophoblast cells to be negative for p63 (**e**), with a Ki-67 labeling index of virtually 0% on dual pan-cytokeratin (red chromogen) and Ki-67 (brown chromogen) stain (**f**)

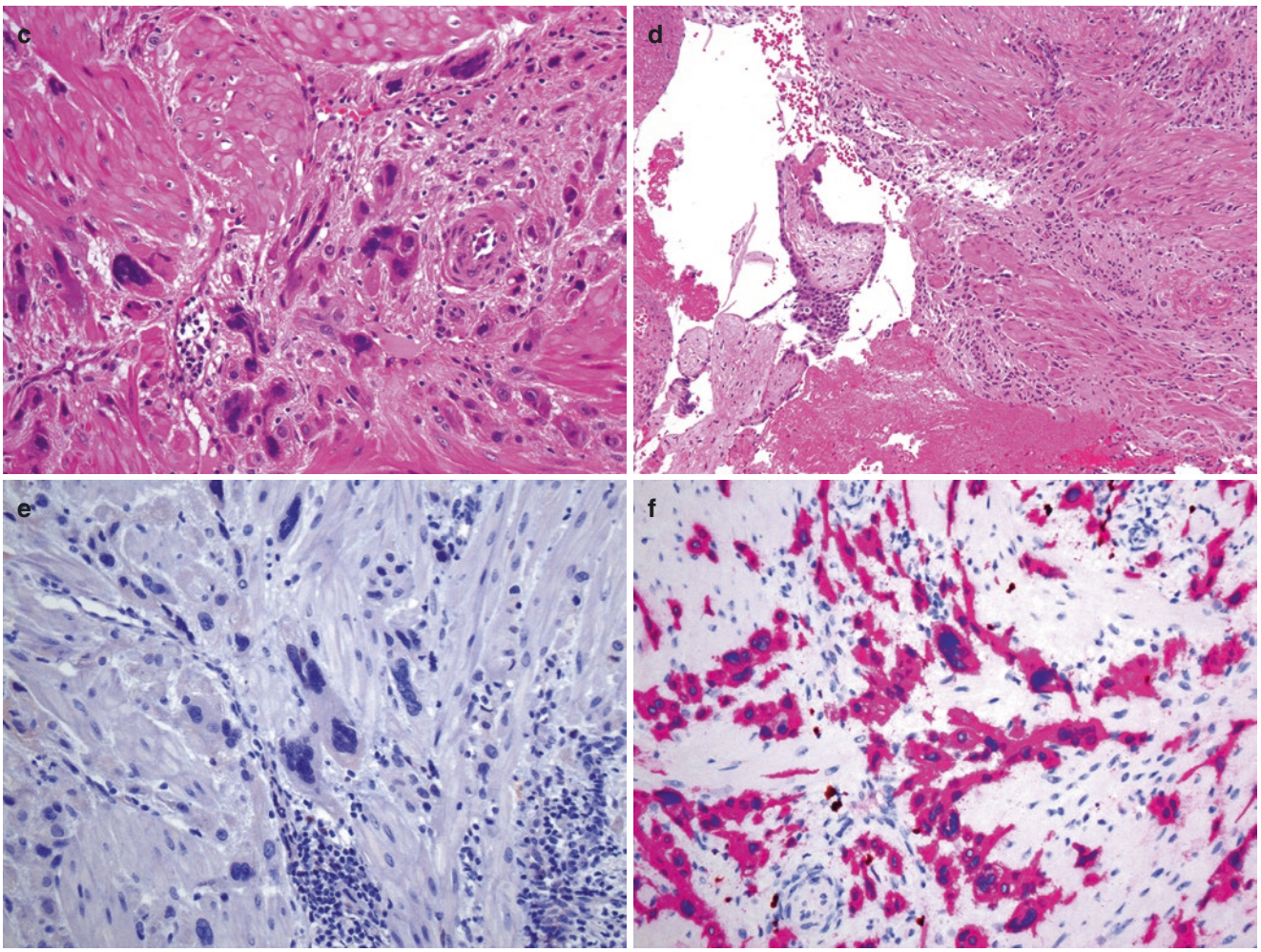

Fig. 12.5 (continued)

12.3.1.7 Prognosis

Patients with untreated choriocarcinoma develop metastases in more than 50% of cases, most commonly to the vagina, lung, liver, brain, or kidney [49]. Cure rates are greater than 90% with chemotherapy [50]. Limited follow-up data for primary cervical gestational choriocarcinoma suggests similar favorable clinical outcomes [51–54].

12.3.2 Placental Site Trophoblastic Tumor

12.3.2.1 Definition

A trophoblastic tumor consisting of neoplastic implantation site intermediate trophoblast cells. The key features of placental site trophoblastic tumor are described in Table 12.5.

12.3.2.2 Synonyms

Atypical choriocarcinoma; syncytioma; chorioepitheliosis; trophoblastic pseudotumor [55].

12.3.2.3 Etiology

Arises from trophoblast with differentiation towards implantation site intermediate trophoblast. Most cases follow normal pregnancy; antecedent complete moles have been reported in 16% of cases and missed abortion in 13% [56].

12.3.2.4 Macroscopy

Expansile to infiltrative, poorly circumscribed, solid masses of 1–10 cm in size, with solid and fleshy, white-tan to light yellow cut surface with focal hemorrhage and necrosis [57]. The tumors may be endophytic or protruding and often extend to serosa, broad ligament, or adnexa.

12.3.2.5 Microscopy

The tumor is composed of central sheets and peripheral cords and nests of round to polygonal intermediate trophoblast with eosinophilic to clear cytoplasm and moderate to marked cytologic atypia. Rare multinucleated cells resembling syncytiotrophoblast are seen. The tumor has infiltrative borders, with the tumor cells separating myometrial smooth muscle

fibers at the periphery. Large nests of tumor cells may replace vascular walls. Associated eosinophilic extracellular matrix may be seen. Necrosis may be present. Mitotic activity is up to 6 per 10 high-power fields (Fig. 12.6).

Immunohistochemically, the tumor shows diffuse staining for hPL, Mel-CAM, MUC-4, HSD3B1, keratins, EMA, GATA3, MUC4, CD10, and HLA-G, with focal staining for PLAP (placental alkaline phosphatase), and no immunoreactivity for p63 and SALL4. Scattered multinucleated cells are positive for β-hCG and inhibin-α. The Ki-67 labeling index is approximately 10–30% [58].

Cytologic features of intermediate trophoblast cells include scattered, small clusters or single large, polygonal cells with ovoid, hyperchromatic nuclei, prominent nucleoli, distinct cell membranes, and abundant eosinophilic or granular cytoplasm in an inflammatory background [59, 60].

Diagnostic Highlights

- Central sheets and peripheral cords and nests of intermediate trophoblast cells
- Round to polygonal tumor cells with eosinophilic to clear cytoplasm and moderate to marked cytologic atypia
- Mitoses up to 6 per 10 high-power fields
- Rare multinucleated cells resembling syncytiotrophoblast
- Infiltrative borders with tumor cells separating myometrial smooth muscle fibers at tumor periphery
- Large nests of tumor cells replacing vascular walls
- Associated eosinophilic extracellular matrix
- Necrosis may be present

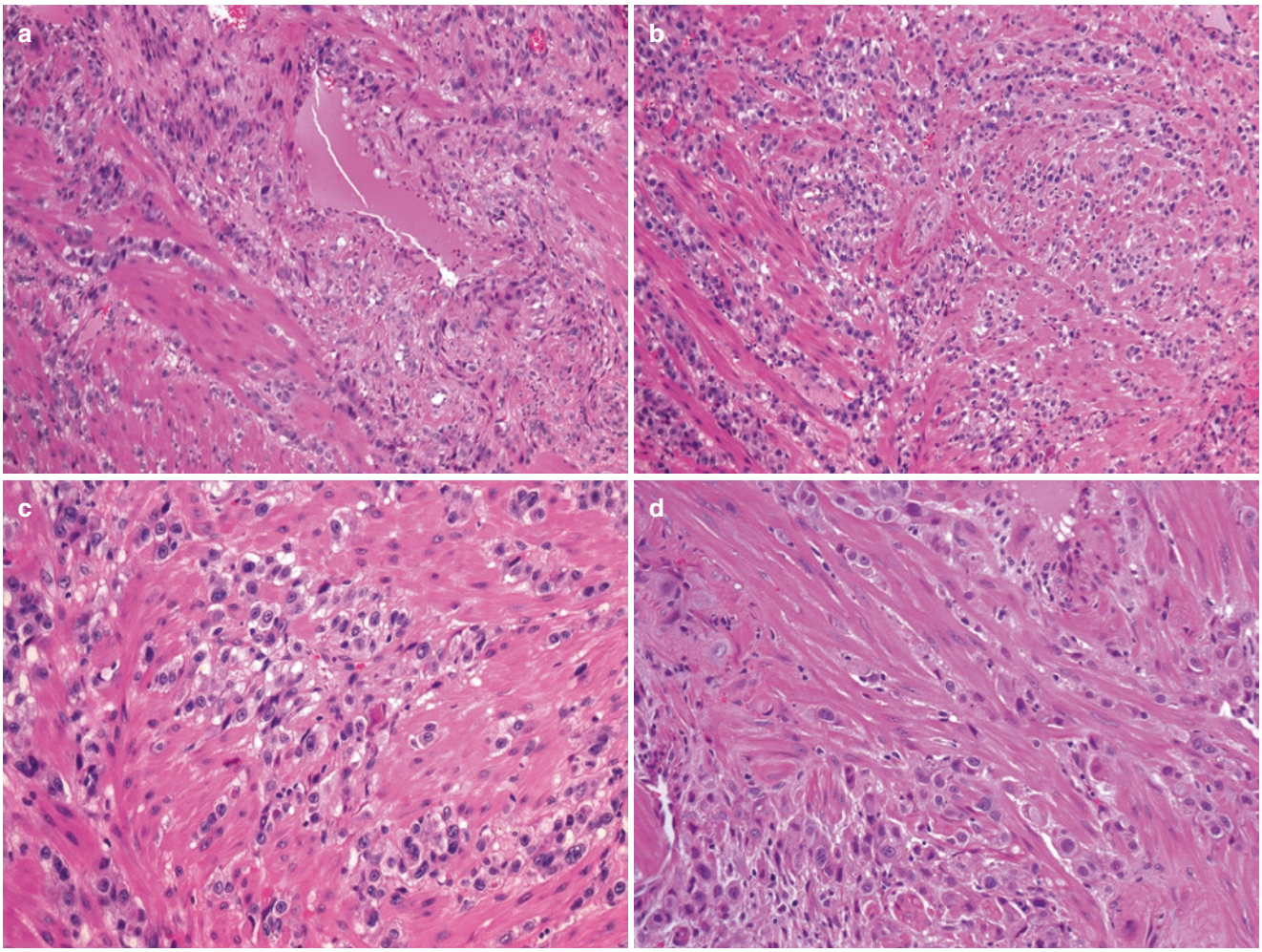

Fig. 12.6 Placental site trophoblastic tumor. (**a–e**), Total hysterectomy specimen with proliferation of atypical epithelioid cells involving myometrium (H&E). The tumor is composed of solid sheets of monomorphic implantation site intermediate trophoblast cells separating myometrial smooth muscle bundles (**a**–**d**). Chorionic villi are not present. The tumor cells replace the vascular walls (**e**). (**f**) A dual pan-cytokeratin (red chromogen) and Ki-67 (brown chromogen) immunohistochemical stain shows a Ki-67 labeling index of 30% in the trophoblastic cells

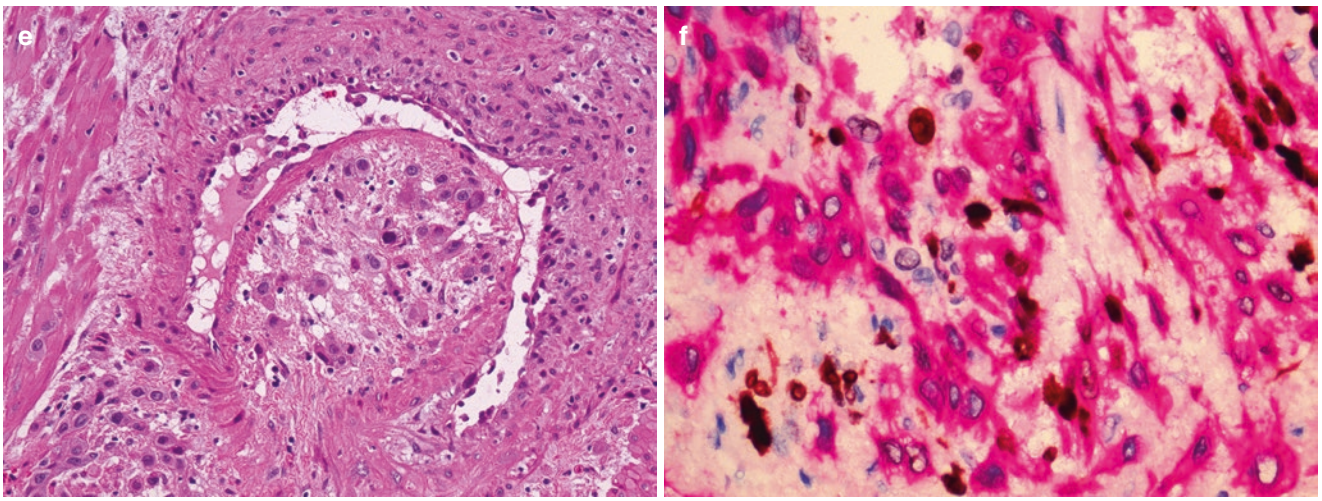

Fig. 12.6 (continued)

12.3.2.6 Differential Diagnosis

Table 12.6 outlines the top differential diagnoses:

- *Placental site nodule* is usually an incidental microscopic lesion, <5 mm in size, composed of single or multiple well-circumscribed, oval nodules or plaques with chorionic-type intermediate trophoblast cells arranged singly or in cords within hyalinized matrix and lacking cytologic atypia or mitotic activity; the center of nodules may be less cellular; Ki-67 < 8% (Fig. 12.7).
- *Atypical placental site nodule is a* larger nodule, measuring 5–10 mm in size; more cellular with cytologic atypia and conspicuous mitotic activity; Ki-67 8–10%; the diagnosis is difficult because of a lack of definitive criteria [56].
- *Exaggerated placental site*. (*See* Fig. 12.5 and Differential Diagnosis in Choriocarcinoma, above.)
- *Epithelioid trophoblastic tumor*. (*See* Differential Diagnosis in Choriocarcinoma, above.)

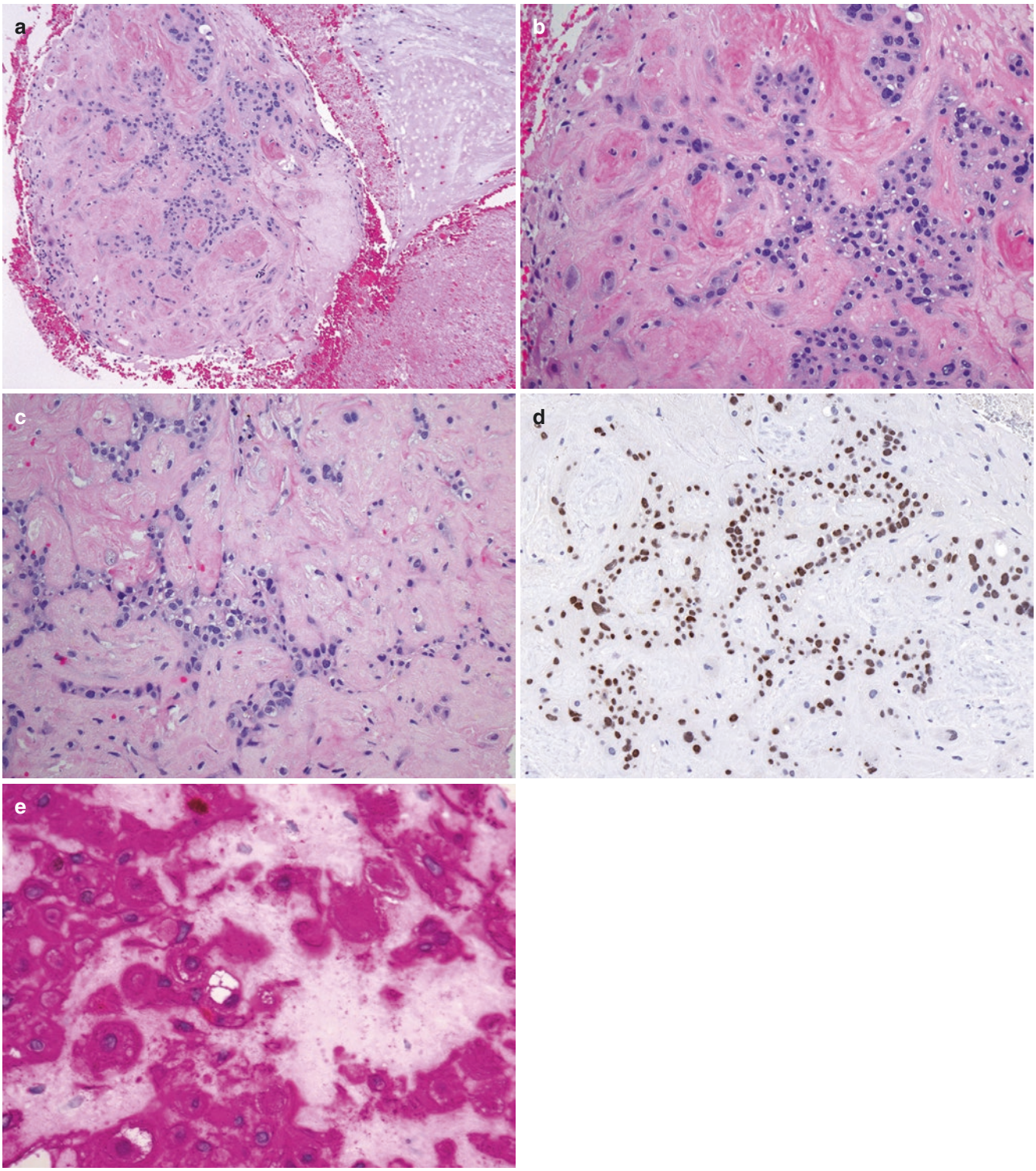

Fig. 12.7 Placental site nodule. (**a–c**), Endocervical curettings for abnormal vaginal bleeding (H&E). There is a single nodule <3 mm in size, with cords of chorionic-type intermediate trophoblast cells embedded within hyalinized matrix, with eosinophilic to clear cell cytoplasm and lacking significant cytologic atypia or mitotic activity. (**d** and **e**), Immunohistochemical stains show the trophoblast cells to be positive for p63 (**d**) with a Ki-67 labeling index of approximately 1% on dual pan-cytokeratin (red chromogen) and Ki-67 (brown chromogen) stain (**e**)

12.3.2.7 Prognosis

Most women with placental site trophoblastic tumor are cured by hysterectomy, but 25–30% of patients may develop recurrent disease, and approximately 50% of those succumb to the disease [61]. Clinical predictors of poor prognosis include high serum β-hCG levels, age 35 years or older, pregnancy at least 48 months antecedent, and previous term pregnancy. Pathologic indicators of adverse outcome are deep myometrial invasion, stage III or IV, extensive coagulative necrosis, high mitotic rate (>5 per 10 high-power fields), and clear cytoplasm. In addition, advanced stage and clear cytoplasm are independent predictors of overall survival; stage and age are independent predictors of recurrence or disease-free survival [57]. Women with stage I disease have a 10-year overall survival probability of 90% (range 77–100%), and do not benefit from adjuvant chemotherapy, whereas women with stage II–IV disease require combined treatment with surgery and chemotherapy. Their 10-year overall survival probability is 52% (range 3–100%) for stage II, and 49% (range 26–72%) for stage III–IV. Only 22% of patients with recurrent or refractory disease are alive beyond 60 months. The only significant independent predictor of overall and recurrence-free survival is time since antecedent pregnancy; a cut-point of 48 months since antecedent pregnancy has been suggested to predict probability of survival with 93% specificity, 100% sensitivity, 100% positive predictive value, and 98% negative predictive value [62].

12.3.3 Epithelioid Trophoblastic Tumor

12.3.3.1 Definition

A trophoblastic tumor consisting of neoplastic chorionic-type intermediate trophoblast cells. The key features of epithelioid trophoblastic tumor are listed in Table 12.5.

12.3.3.2 Synonyms

Atypical choriocarcinoma; "multiple nodules of intermediate trophoblast" [63–65].

12.3.3.3 Etiology

Arises from trophoblast with differentiation towards chorionic-type intermediate trophoblast [66, 67]. Most cases (67%) follow normal term pregnancy; hydatidiform moles and spontaneous abortion have each been reported in 16% of cases. Occurrence in premenopausal and postmenopausal women is common [68]. Malignant transformation from an atypical placental site nodule has been suggested [69, 70].

12.3.3.4 Macroscopy

Expansile solid mass measuring 0.5–5 cm, with endophytic or exophytic growth. The tumor may be solid or cystic on cut section, with hemorrhage and necrosis. Approximately 50% of cases arise from the uterine cervix or lower uterine segment [71].

12.3.3.5 Microscopy

The tumor has pushing borders and consists of well-circumscribed sheets, nests, and cords of intermediate trophoblast cells and a central small vessel. Extensive or "geographic" necrosis is often present. Eosinophilic extracellular hyaline-like matrix material may mimic keratin, leading to misdiagnosis as carcinoma in some cases. The tumor may colonize the overlying cervical epithelium, mimicking HSIL. The tumor cells exhibit mild to moderate nuclear atypia, prominent nucleoli, and up to 9 mitotic figures per 10 high-power fields (Fig. 12.8). The tumor periphery may show scattered, decidualized, benign stromal cells [71].

Immunohistochemically, the tumor is diffusely positive for p63, PLAP, keratins (pan-cytokeratin, CK18), EMA, inhibin-α, HLA-G, GATA3, H3D3B1, HLA-G, cyclin E, and CD10; focally positive for hPL, Mel-CAM and β-hCG; and negative for SALL4; Ki-67 10–25% [58].

Cytologic features are those of intermediate trophoblastic cells. (*See* Placental site trophoblastic tumor, above.) A differential diagnosis between different gestational trophoblastic diseases cannot be made on the basis of cytologic examination [59, 60].

Diagnostic Highlights

- Sheets, nests, and cords of intermediate trophoblast cells
- Rare syncytiotrophoblast
- Hyaline-like material
- May colonize cervical mucosal epithelium
- Mild to moderate cytologic atypia with prominent nucleoli
- Mitoses up to 9 per 10 high-power fields
- Decidualized stromal cells at tumor periphery (variable)
- "Geographic" necrosis

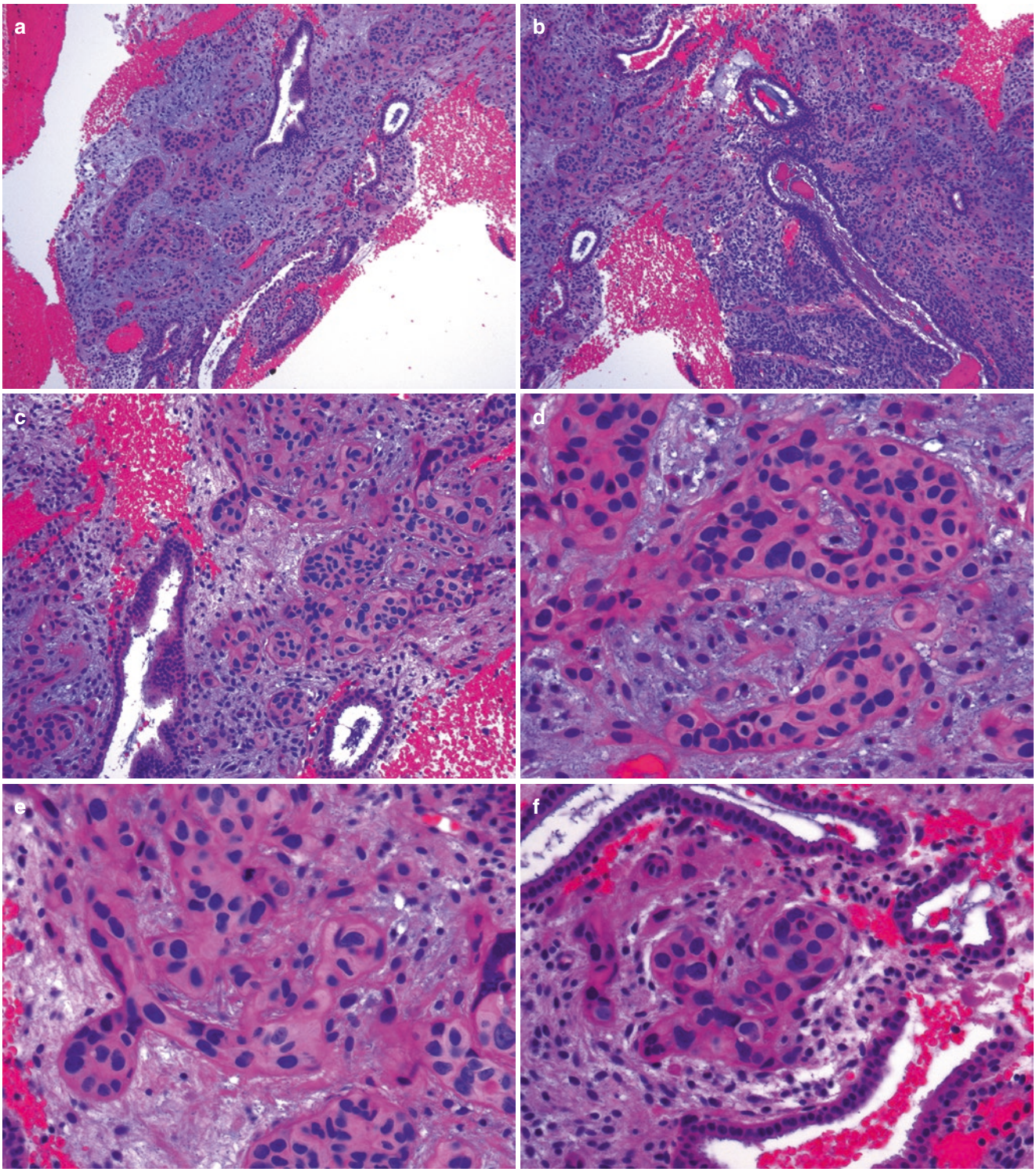

Fig. 12.8 Epithelioid trophoblastic tumor. (**a–i**), Cervical biopsy with fragments of endocervical tissue containing nests and cords of epithelioid cells surrounding benign endocervical glands (H&E). The cells exhibit mild to moderate nuclear atypia (**a–i**) and scattered mitotic figures (**e, g, h**). Nodular growth pattern with characteristic "geographic" necrosis (**i**) (courtesy of Dr. R. Soslow). Chorionic villi are not present. (**j** and **k**), Immunohistochemical stains show the tumor cells to be positive for p63 (**j**), CK18, and PLAP, with a Ki-67 labeling index of approximately 20% on dual pan-cytokeratin (red chromogen) and Ki-67 (brown chromogen) stain (**k**)

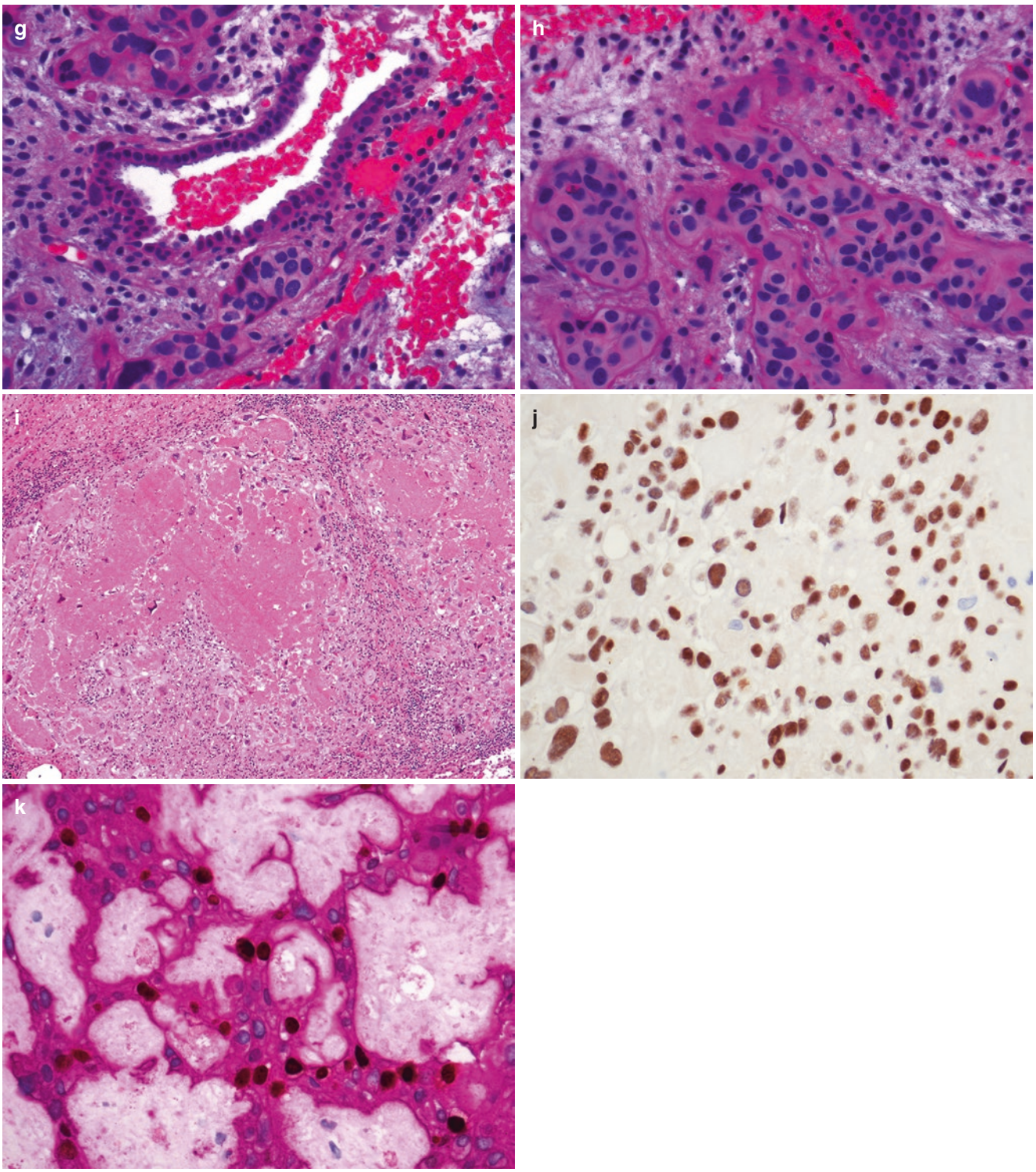

Fig. 12.8 (continued)

12.3.3.6 Differential Diagnosis

Table 12.6 outlines the top differential diagnoses:

- *Placental site nodule* and a*typical placental site nodule.* (*See* Differential Diagnosis in Placental Site Trophoblastic Tumor, above.)
- *Squamous cell carcinoma* may be associated with HSIL (p16 and HPV-positive), features of squamous differentiation such as keratinization or intercellular bridges; lacking decidualized benign stromal cells at tumor periphery; negative for inhibin-α, HLA-G, Mel-CAM, hPL, and usually CK18.
- *Choriocarcinoma* exhibits mononuclear trophoblast surrounded by syncytiotrophoblast; shows extensive necrosis and hemorrhage; Ki-67 > 90%.
- *Epithelioid leiomyosarcoma* is positive for smooth muscle markers; negative for markers of trophoblastic differentiation.
- *Poorly differentiated carcinoma with trophoblastic differentiation*. (*See* Differential Diagnosis in Choriocarcinoma, above.)

12.3.3.7 Prognosis

Similar to placental site trophoblastic tumor, 25% of patients with epithelioid trophoblastic tumor develop metastases with a mortality rate of 10% [72]. The survival is nearly 100% for nonmetastatic disease and 50–60% in metastatic disease. The only unfavorable histologic feature has been shown to be a high mitotic count (>6 per 10 high power fields) [73].

12.4 Lymphoid Tumors

12.4.1 Definition

Malignant neoplasms composed of lymphoid cells.

12.4.2 Synonyms

Lymphoma.

12.4.3 Etiology

Cervical lymphoid tumors have a hematopoietic origin and can be part of a systemic process or present primarily with cervical involvement. The most common type is B-cell lymphoma. A systematic review from 2014 identified 143 cases of primary diffuse large B-cell lymphoma (DLBCL) of the uterus, of which 108 (75.5%) had cervical involvement [74], including case reports and case series [74–79]. Three additional cases were also published much earlier [80–82]. The second-most-common type of primary cervical lymphoma is follicular lymphoma (FL). The cervix also may be involved by chronic lymphocytic leukemia/small lymphocytic lymphoma (CLL/SLL), the most common adult leukemia, which is characterized by lymphocytosis due to the accumulation of small B lymphocytes in the blood, bone marrow, and lymphoid tissues. These lymphomas are often diagnosed incidentally in asymptomatic patients; rarely, diagnosis is based on gynecologic manifestations such as vaginal bleeding or abnormal colposcopic findings [78, 79, 83–89]. Rare cervical Burkitt lymphomas, extranodal NK/T-cell lymphomas, marginal zone lymphomas, mucosa-associated lymphoid tissue–type lymphomas, and Hodgkin lymphomas have also been described [78, 90–94]. The key features of lymphoid tumors involving the cervix are described in Table 12.7.

Table 12.7 Key features of the most common cervical lymphoid tumors

	Diffuse large B-cell lymphoma	Follicular lymphoma	Chronic lymphocytic leukemia/small lymphocytic lymphoma
Clinical presentation	Asymptomatic Abnormal cervical cytology Abnormal bleeding Cervical mass	Asymptomatic Abnormal cervical cytology Abnormal bleeding Cervical mass	Asymptomatic Abnormal cervical cytology Abnormal bleeding Cervical mass
Macroscopy	Sharply demarcated bulky masses "Barrel-shaped" cervix Submucosal lesions with intact overlying epithelium Polypoid single or multinodular lesions Exophytic mass Mean tumor size 4 cm Fleshy, rubbery or firm, homogenous, white-tan to yellow cut surface May extend into deep soft tissues and surrounding organs	Sharply demarcated bulky masses "Barrel-shaped" cervix Submucosal lesions with intact overlying epithelium Polypoid single or multinodular lesions Exophytic mass Mean tumor size 4 cm Fleshy, rubbery or firm, homogenous, white-tan to yellow cut surface May extend into deep soft tissues and surrounding organs	Sharply demarcated bulky masses "Barrel-shaped" cervix Submucosal lesions with intact overlying epithelium Polypoid single or multinodular lesions Exophytic mass Mean tumor size 4 cm Fleshy, rubbery or firm, homogenous, white-tan to yellow cut surface May extend into deep soft tissues and surrounding organs

(continued)

Table 12.7 (continued)

	Diffuse large B-cell lymphoma	Follicular lymphoma	Chronic lymphocytic leukemia/small lymphocytic lymphoma
Microscopy	Narrow band of uninvolved stroma beneath surface epithelium Deep extension into cervical wall with pushing borders Sparing of endocervical glands Prominent sclerosis Rarely ulceration or necrosis Sheets or cords of dyscohesive lymphoid cells, storiform growth, or spindle-shaped tumor cells Tumor cells with large, vesicular, oval, irregular and multilobated nuclei with coarse to vesicular chromatin and brisk mitotic activity Associated crush artifact	Narrow band of uninvolved stroma beneath surface epithelium Deep extension into cervical wall with pushing borders Sparing of endocervical glands Prominent sclerosis Rarely ulceration or necrosis Nodular growth of monomorphous, large follicles lacking mantle zone and extending into the cervical wall and paracervical soft tissue Admixture of centrocytes and centroblasts Some tingible body macrophages	Narrow band of uninvolved stroma beneath surface epithelium Deep extension into cervical wall with pushing borders Sparing of endocervical glands Vaguely nodular growth pattern with alternating dark zones of mature lymphocytes and lighter zones containing prolymphocytes and paraimmunoblasts admixed with small lymphocytes, termed *proliferation centers* Inconspicuous cytologic atypia and mitotic activity
Immunohistochemistry	*Positive:* Pan B-markers (CD20, CD19, CD79a) Bcl-6 CD10 Bcl-2 CD5 MUM1 CD43	*Positive:* Pan B-markers (CD20, CD19, CD79a) Bcl-6, Bcl-2, and CD10 in follicles CD21 or CD23 in follicular dendritic cell meshworks *Negative:* CD5 CD43 Cyclin-D1	*Positive:* Pan B-markers (CD20, CD19, CD79a) CD5 CD23 PAX5 CD43 CD11c

Bcl-2 B-cell lymphoma, *MUM1* Multiple Myeloma 1

12.4.4 Macroscopy

Lymphomas tend to form sharply demarcated, bulky masses and may cause circumferential enlargement of the cervix ("barrel-shaped" cervix). Gross features include submucosal lesions with intact overlying epithelium [95, 96], polypoid single or multinodular lesions, and exophytic masses [95, 97, 98]. The mean tumor diameter is 4 cm. The cut surface of the tumors is often fleshy, rubbery, or firm with homogenous white-tan to yellow appearance [95]. Extension into deep soft tissues and surrounding organs is not uncommon.

12.4.5 Microscopy

Lymphomas tend to show a narrow band of uninvolved stroma beneath surface epithelium, and deep extension into the cervical wall with pushing borders, sparing of endocervical glands, prominent sclerosis, and rarely ulceration or necrosis. Histologic features of relatively common lymphomas are summarized below:

Cervical DLBCL is often associated with deep infiltration and marked sclerosis [90, 98, 99], with sheets or cords of dyscohesive lymphoid cells, storiform growth, or spindle-shaped tumor cells [95]. Tumors with spindle cell morphology have been termed "spindle cell variant" [100] or "sarcomatoid variant" [101] and may mimic sarcoma. Rarely, ulceration or necrosis may be seen. The neoplastic cells exhibit large vesicular, oval, irregular, and multilobated nuclei with coarse to vesicular chromatin and brisk mitotic activity (Fig. 12.9). Associated crush artifact is common.

FL typically shows nodular growth of monomorphous large follicles lacking a mantle zone and extending into the

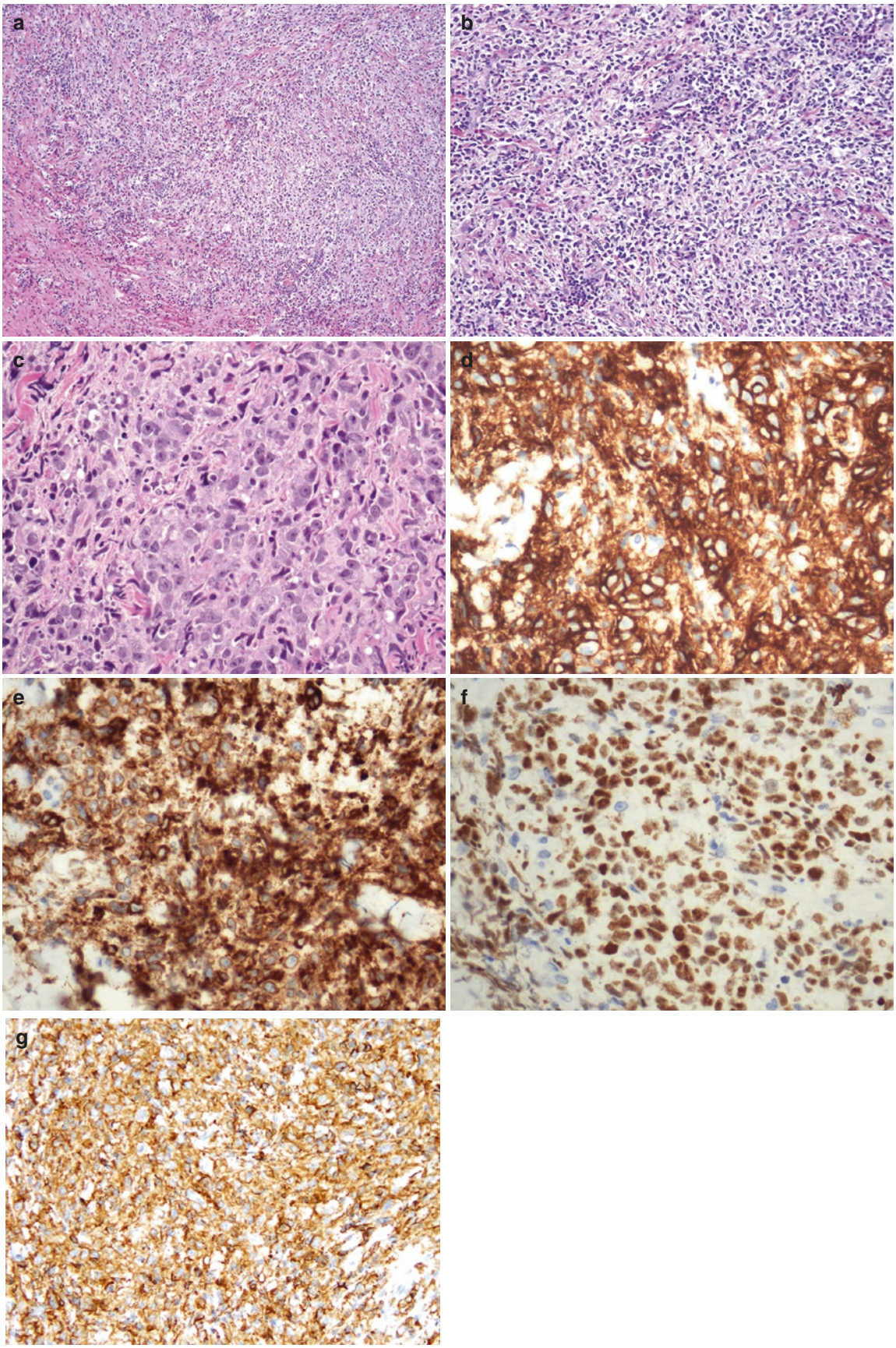

Fig. 12.9 Diffuse large B-cell lymphoma. (**a–c**), Total hysterectomy with diffuse sheets of neoplastic cells involving the middle and outer thirds of the cervical wall (H&E). The tumor cells exhibit large vesicular, oval to spindle-shaped, irregular, and multilobated nuclei with coarse to vesicular chromatin and brisk mitotic activity (**c**). The background stroma is sclerotic (**a, b**). (**d–g**), Immunohistochemical stains show the tumor to be positive for CD20 (**d**), Bcl-2 (**e**), Bcl-6 (**f**), and CD10 (**g**). The patient has no prior history of hematolymphoid disease

cervical wall and paracervical soft tissue (Fig. 12.10). Cervical FL frequently shows sclerosis. The neoplastic cells are predominantly small lymphoid cells (centrocytes) admixed with larger lymphoid cells (centroblasts). Occasional tingible body macrophages may be seen. FL is graded based on the number of centroblasts per high-power field of view:

- Grade 1: 0–5
- Grade 2: 6–15
- Grade 3: >15, further categorized as grade 3A (centrocytes admixed with centroblasts) and 3B (sheets of centroblasts with rare or no centrocytes)

Grades 1 and 2 are considered low-grade. All three grades have been described in the cervix [78, 90, 91].

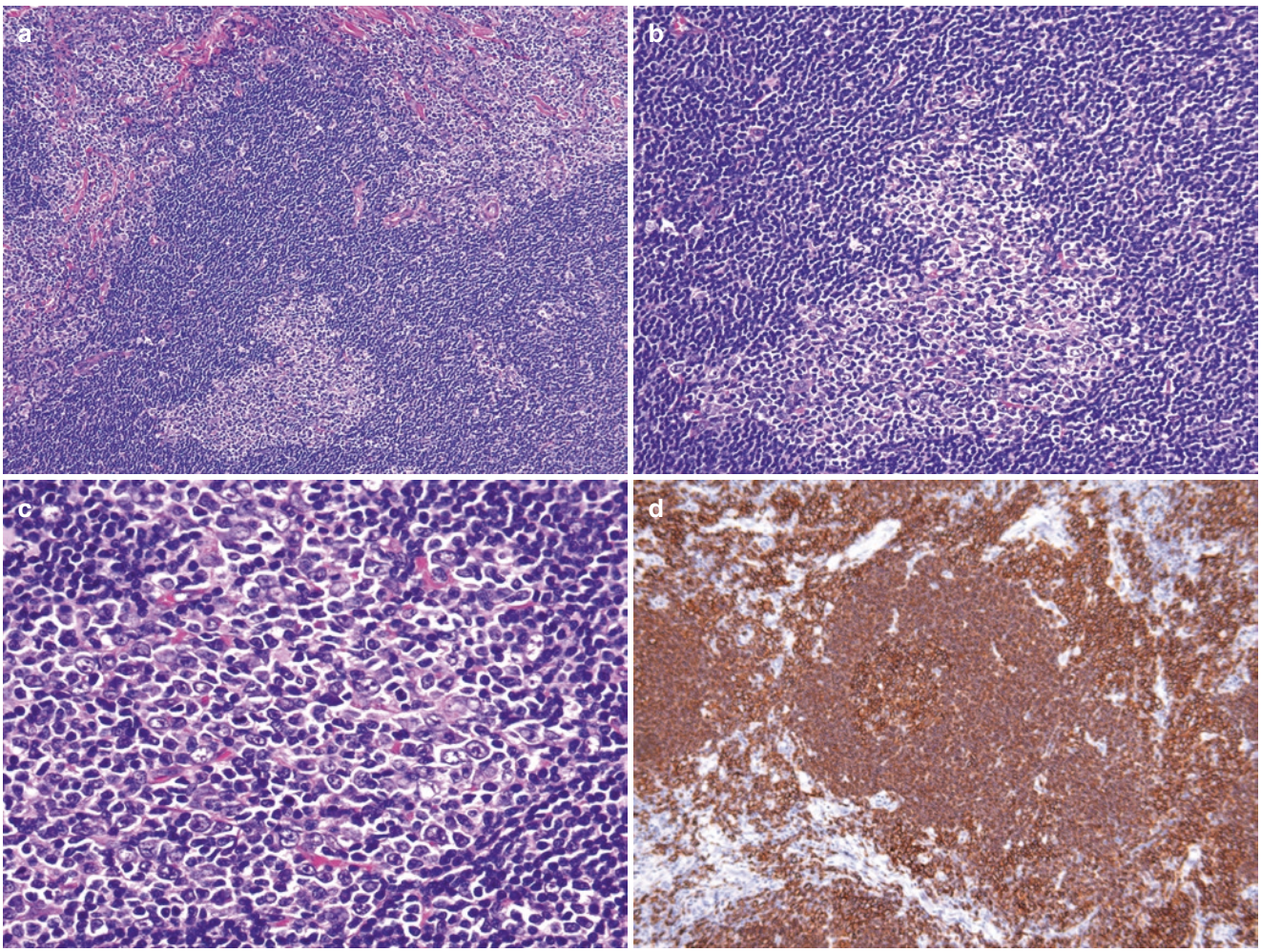

Fig. 12.10 Follicular lymphoma. (**a–c**), Total hysterectomy with an extensive lymphoid infiltrate (H&E) with prominent germinal centers and composed of a mixture of variably sized cells with angulated nuclei and condensed chromatin (centrocytes) and larger cells with oval or multilobated nuclei, vesicular chromatin, and several nucleoli (centroblasts). (**d–g**), Immunohistochemical stains show the tumor to be positive for CD20 (**d**) with expression of Bcl-2 (**e**), Bcl-6 (**f**), and CD21 (**g**) in the neoplastic germinal centers, and negative for CD5, CD43 and cyclin D1. The patient has no prior history of hematolymphoid disease

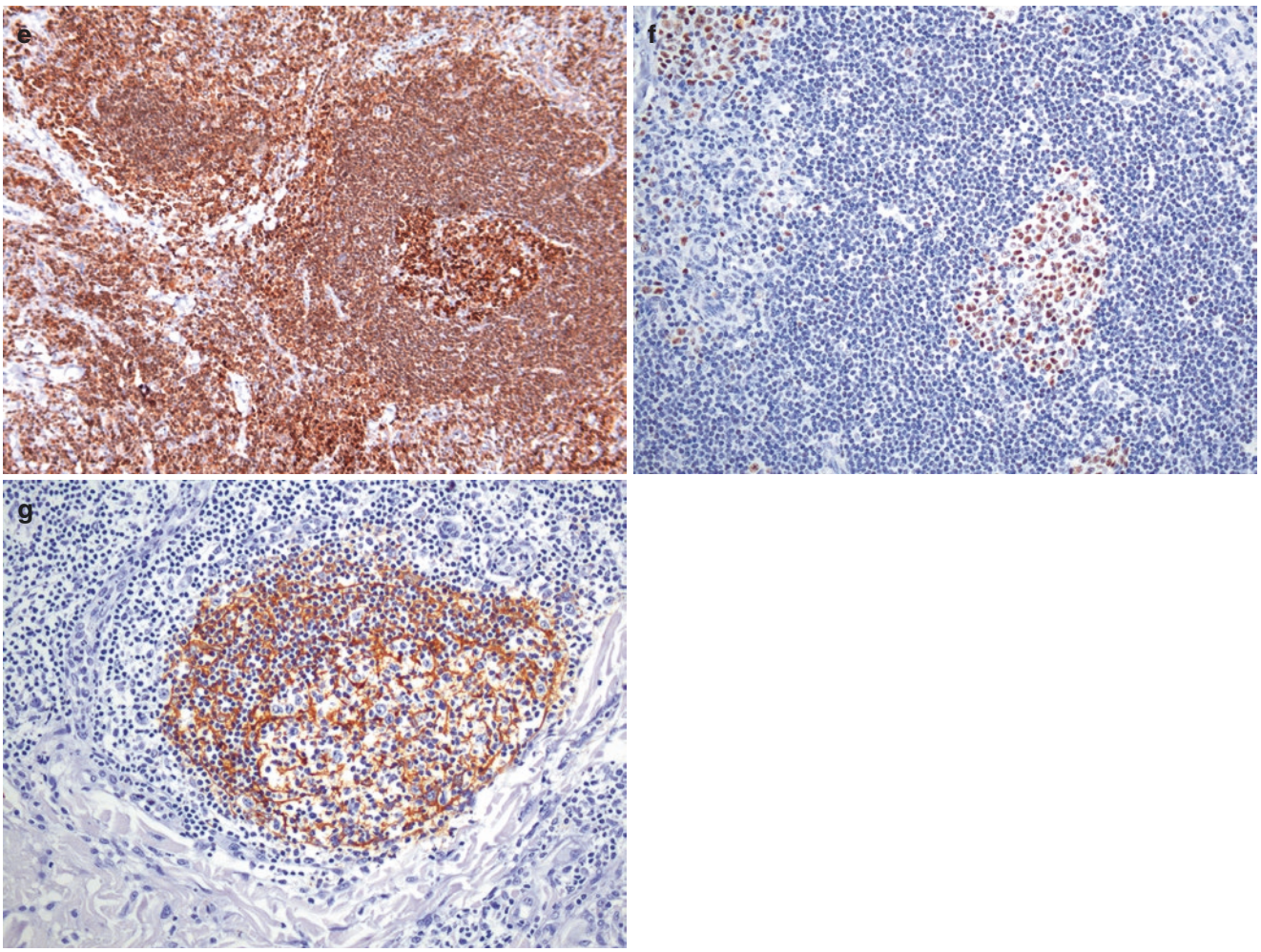

Fig. 12.10 (continued)

CLL/SLL is characterized by a vaguely nodular growth pattern with alternating dark zones of mature lymphocytes and lighter zones, termed a *proliferation center*, containing prolymphocytes (medium-sized cells with dispersed chromatin and small nucleoli) and paraimmunoblasts (medium to large cells with round to oval nuclei, dispersed chromatin, and central eosinophilic nucleoli) admixed with small lymphocytes (clumped chromatin, round nuclei, occasional small nucleoli) (Fig. 12.11). Cytologic atypia and mitotic activity are usually inconspicuous.

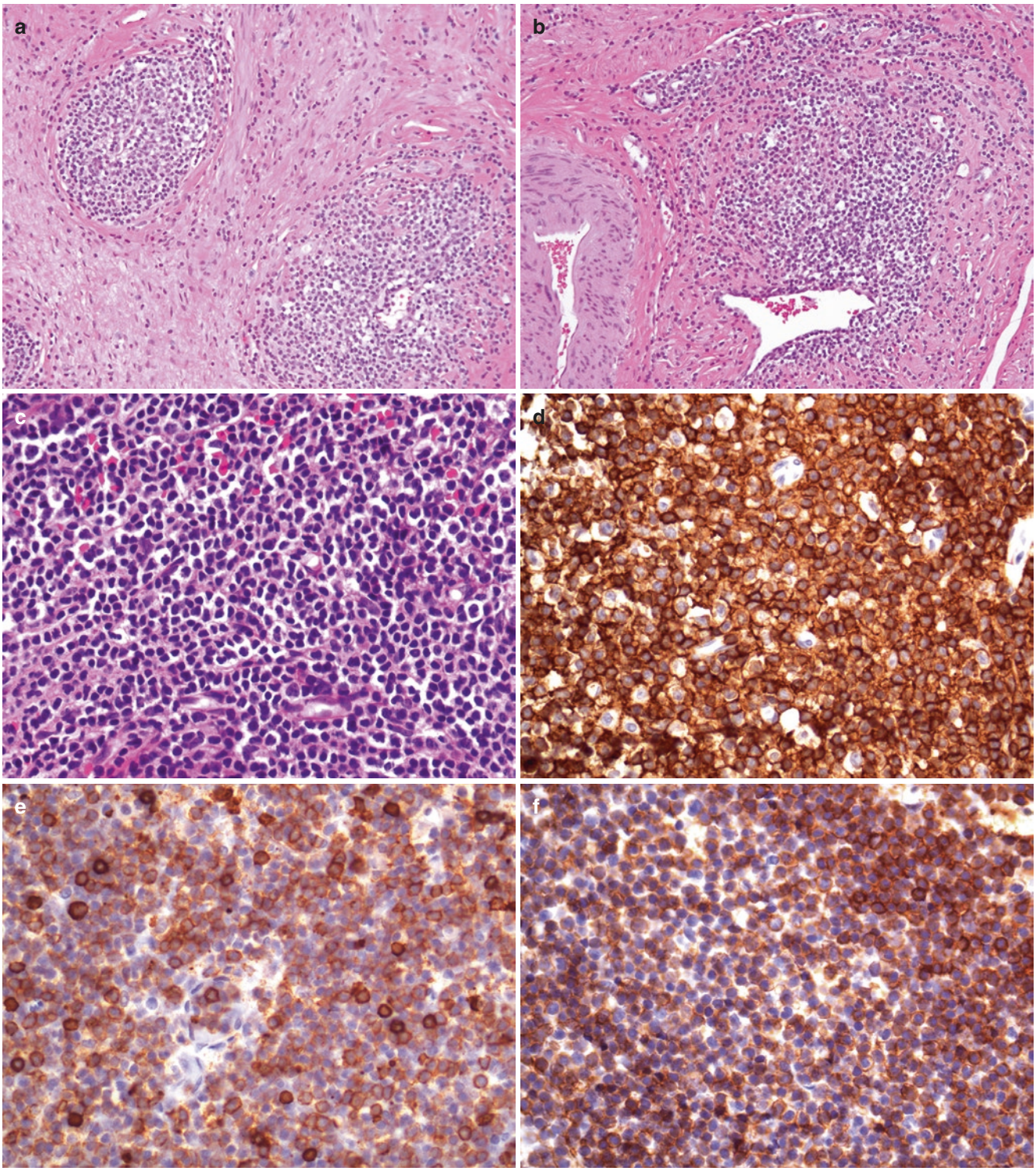

Fig. 12.11 Chronic lymphocytic leukemia/small lymphocytic lymphoma. (**a–c**), Cervical cone biopsy with nodular and perivascular lymphoid infiltrates (H&E). The lymphoid cells show small to medium-sized cells with dispersed chromatin and generally inconspicuous nucleoli (**c**). (**d–f**), Immunohistochemical stains show the lymphoid cells to be positive for CD20 (**d**), CD5 (**e**), CD23 (**f**), and CD43, and negative for cyclin D1. The patient has a prior history of chronic lymphocytic leukemia

Immunohistochemistry can help with diagnosis:

- DLBCL is positive for pan B-cell markers, in addition to Bcl-6, CD10, Bcl-2, CD5, MUM1, and CD43.
- FL is positive for pan B-cell markers; neoplastic follicles express Bcl-6, Bcl-2, and CD10. CD5, CD43, and cyclin D1 are usually negative; follicular dendritic cell meshworks are highlighted by CD21 or CD23.
- CLL/SLL is positive for pan B-cell markers with co-expression of CD5 and CD23; CD43, PAX5 and CD11c may be positive.

Some cytogenetic findings are also characteristic of these lymphomas [102]:

- DLBCL: 3q27 abnormalities involving *BCL6* are found in 30% of cases, t(14;18) involving *BCL2* in 20–30%, and *MYC* rearrangement in 10%.
- FL: IgH and IgL gene rearrangements, t(14;18)(q32;q21) with *IGH-BCL2* rearrangement is found in 70–95% of cases.
- CLL/SLL: *IGH* and *IGL* gene rearrangements, trisomy 12, del 13q, del(17p), or del(11q) may be present.

Cytologically, lymphomas typically show a dispersed population of monotonous but atypical lymphocytes, sometimes with obscuring blood and inflammation in the background.

- DLBCL is comprised of cells with a high nuclear-cytoplasmic ratio, some with prominent nucleoli, in a bloody background.
- FL exhibits a mixture of centrocytes (variably sized cells with cleaved or angulated nuclei and condensed chromatin) and centroblasts (large cells with noncleaved oval or multilobated nuclei, vesicular chromatin, and several nucleoli), often with germinal center aggregates.
- CLL/SLL is primarily composed of small lymphocytes with clumped chromatin and scattered prolymphocytes (medium-sized cells with dispersed chromatin and conspicuous nucleoli) and paraimmunoblasts (medium to large cells with round to oval nuclei, dispersed chromatin, and conspicuous central nucleoli).

Diagnostic Highlights

All lymphomas

- Mass lesion
- Narrow band of uninvolved stroma beneath surface epithelium
- Deep extension into cervical wall with pushing borders
- Sparing of endocervical glands
- Prominent sclerosis
- Rarely ulceration or necrosis

DLBCL

- Sheets or cords of dyscohesive lymphoid cells and, less commonly, storiform growth or spindle-shaped tumor cells
- Tumor cells with large, vesicular, oval, irregular and multilobated nuclei with coarse to vesicular chromatin and brisk mitotic activity
- Associated crush artifact

FL

- Nodular growth of monomorphous, large follicles lacking a mantle zone and extending into the cervical wall and paracervical soft tissue
- Admixture of centrocytes and centroblasts
- Occasional tingible body macrophages

CLL/SLL

- Vaguely nodular growth pattern with alternating dark zones of mature lymphocytes and lighter zones containing prolymphocytes and paraimmunoblasts admixed with small lymphocytes, termed *proliferation centers*
- Inconspicuous cytologic atypia and mitotic activity

12.4.6 Differential Diagnosis

Secondary involvement of the uterine cervix by a variety of lymphomas in the setting of systemic disease is significantly more common than primary cervical lymphomas [90, 95, 97, 103]. In such cases, clinical correlation is essential in ruling out systemic involvement. Cervical lymphomas should also be differentiated from poorly differentiated primary neoplasms. In general, the absence of an associated intraepithelial lesion, diffuse and infiltrative growth pattern, positive lymphoid markers, and/or a prior history of lymphoma should raise suspicion and trigger additional work-up for lymphomas in cervical specimens.

Table 12.8 lists the top differential diagnoses:

- *Secondary involvement by systemic disease* may be suspected based on clinical history of systemic lymphoma or concurrent tumor in lymph nodes and/or extragenital organs.
- *Reactive lymphoid infiltrate* should be differentiated from CLL/SLL based on superficial band-like infiltrate composed of B-cells and T-cells and neutrophils; no mass lesion, infiltrative growth or sclerosis; common surface erosion; in addition, a history of CLL/SLL, recent lymphocytosis, older age, and/or CD20-positive lymphocytic infiltrates should raise suspicion for cervical involvement by CLL/SLL.

- *Reactive lymphoid follicles* show central polarized germinal centers with dark and light zones surrounded by peripheral, sharply demarcated mantle zones; lack of coalescing follicles; germinal centers positive for Bcl-6 and CD10 but negative for Bcl-2.
- *Mantle cell lymphoma* is composed of intermediate-size nuclei with irregular contours; usually negative for CD23; positive for pan B-cell markers, CD5, cyclin D1 and t(11;14)(q13;q32).
- *Marginal zone B-cell lymphoma* is characterized by common bone marrow involvement, sometimes with lymphocytosis; atypical centrocyte-like cells (histiocytoid lymphocytes with round to reniform or cleaved nuclei, contrasted against dark-staining lymphocytes) infiltrating around reactive B-cell follicles and interfollicular areas; positive for pan B-cell markers, and CD5 in 20%; negative for CD5 and cyclin D1.
- *Small cell neuroendocrine carcinoma* is composed of nests, islands, or sheets of cohesive tumor cells with salt-and-pepper chromatin; positive for high-risk HPV, p16, epithelial and neuroendocrine markers; variable expression of TTF-1, aberrant p53; common loss of Rb.
- *Lymphoepithelial-like squamous cell carcinoma* exhibits cohesive nests of cells; positive for epithelial markers, p63, and p40; negative for lymphoid markers.
- *Malignant melanoma* is positive for melanocytic markers; negative for lymphoid markers.
- *High-grade endometrial stromal sarcoma* may be positive for CD10, ER and PR in some types and negative in others; negative for lymphoid markers.

Table 12.8 Differential diagnosis of lymphoid and myeloid tumors involving the cervix

			Ancillary studies	
	Clinical history	Microscopy	Positive	Negative
Diffuse large B-cell lymphoma	No lymphoma elsewhere	Sheets or cords of dyscohesive lymphoid cells, storiform growth, or spindle-shaped tumor cells; tumor cells with large vesicular, oval, irregular, and multilobated nuclei with coarse to vesicular chromatin and brisk mitotic activity; associated crush artifact	CD20, CD19, CD79a, Bcl-6, CD10, Bcl-2, CD5, MUM1, CD43	Cyclin D1
Follicular lymphoma	No lymphoma elsewhere	Nodular growth of monomorphous, large follicles lacking mantle zone and extending into the cervical wall and paracervical soft tissue; admixture of centrocytes and centroblasts, ± tingible body macrophages	CD20, CD19, and CD79a; follicles with Bcl-6, Bcl-2, CD10, follicular dendritic cell meshworks with CD21 or CD23	CD5, CD43, cyclin D1
Chronic lymphocytic leukemia/small lymphocytic lymphoma	No lymphoma elsewhere	Vaguely nodular growth pattern with alternating dark zones of mature lymphocytes and lighter zones containing prolymphocytes and paraimmunoblasts admixed with small lymphocytes, termed *proliferation centers*; bland cytology and no mitotic activity	CD19, CD20, CD79a, CD5, CD23, PAX5, CD43, CD11c	Cyclin D1
Myeloid sarcoma	No hematolymphoid neoplasm elsewhere	Diffuse sheets of primitive, monotonous myeloid cells; tumor cells with medium to large, oval, irregular, reniform or folded nuclei, fine chromatin, prominent nucleoli, and scant to moderate cytoplasm; admixed maturing cells with recognizable myeloid differentiation, lymphocytes, tingible body macrophages and megakaryocytes; sclerosis and vascular wall involvement; rarely pseudo-alveolar, trabecular, or cord-like patterns	CD68, CD43, CD68, CD43, CD33, CD117, myeloperoxidase, lysozyme; variable CD34, CD13, CD14, CD15, CD45, antitrypsin, antichymotrypsin	Cyclin D1
Secondary involvement by systemic disease	Systemic lymphoma, concurrent tumor in lymph nodes and/or extragenital organs	Same as systemic disease	Same as systemic disease	Same as systemic disease
Reactive lymphoid infiltrate	None	Superficial band-like infiltrate composed of B-cells and T-cells and neutrophils; no mass lesion, infiltrative growth or sclerosis; common surface erosion	CD20, CD3, CD45	Cyclin D1

Table 12.8 (continued)

	Clinical history	Microscopy	Ancillary studies	
			Positive	Negative
Reactive lymphoid follicles	None	Central polarized germinal centers with dark and light zones surrounded by peripheral, sharply demarcated mantle zones; lack of coalescing follicles	Germinal centers positive for Bcl-6 and CD10	Germinal centers negative for Bcl-2
Mantle cell lymphoma	No lymphoma elsewhere	Intermediate-size nuclei with irregular contours	CD20, CD19, CD5, cyclin D1, t(11;14)	CD23, CD10
Marginal zone B-cell lymphoma	Common bone marrow involvement, sometimes with lymphocytosis	Atypical centrocyte-like cells (histiocytoid lymphocytes with round to reniform or cleaved nuclei, contrasted against dark-staining lymphocytes) that infiltrate around reactive B-cell follicles in a marginal zone distribution with spread into the interfollicular area	CD19, CD20, CD79a, CD22, CD5 in 20%	Cyclin D1, CD5
Small cell neuroendocrine carcinoma	Cervical cancer, positive HPV	Nests, islands, or sheets of cohesive tumor cells with salt-and-pepper chromatin	p16, cytokeratin, chromogranin, synaptophysin, high-risk HPV, variable expression of TTF-1, aberrant p53, common loss of Rb	Lymphoid markers
Lymphoepithelial-like squamous cell carcinoma	Cervical cancer	Cohesive nests of epithelioid cells	Cytokeratin, p63, p40, p16, high-risk HPV	Lymphoid markers
Malignant melanoma	Melanoma	Epithelioid cells with brisk mitoses and prominent nucleoli	S100, HMB-45, Melan-A/MART-1, MITF, SOX10	Lymphoid markers
High-grade endometrial stromal sarcoma	Sarcoma	High-grade round cells with nested or pseudo-glandular patterns separated by thin-walled vessels (YWHAE type); brisk mitoses; necrosis	±CD10, ER, PR	Lymphoid markers

Bcl-2 B-cell lymphoma, *ER* estrogen receptor, *HPV* human papillomavirus, *HMB-45* human melanoma black 45, *MART-1* melanoma antigen recognized by T cells, *MITF* microphthalmia transcription factor, *MUM1* MUltiple Myeloma 1, *PAX5* paired box 5, *PR* progesterone receptor, *Rb* retinoblastoma, *SOX10* SRY-related HMG-box 10, *TTF-1* thyroid transcription factor 1

12.4.7 Prognosis

Primary cervical lymphomas are usually localized and have a favorable clinical outcome. High-stage disease is associated with a less favorable outcome [104]. Germinal center B-cell–like DLBCL subtype is associated with better overall survival [105].

12.5 Myeloid Tumors

12.5.1 Definition

Malignant neoplasm of myeloid origin. Myeloid sarcoma is a mass-forming lesion composed of primitive myeloid cells. The key features of myeloid sarcoma involving the cervix are described in Table 12.9.

Table 12.9 Key features of cervical myeloid sarcoma

Clinical presentation
• Asymptomatic
• Abnormal bleeding
• Cervical mass
• Systemic symptoms
Macroscopy
• Diffuse enlargement
• Nodularity
• Cervical mass
Microscopy
• Diffuse sheets of primitive monotonous myeloid cells
• Tumor cells with medium to large, oval, irregular, reniform or folded nuclei, fine chromatin, prominent nucleoli, and scant to moderate cytoplasm
• Admixed maturing cells with recognizable myeloid differentiation, lymphocytes, tingible body macrophages and megakaryocytes
• Sclerosis and vascular wall involvement
• Rarely, pseudo-alveolar, trabecular, or cord-like patterns
Immunohistochemistry
• Positive:
– CD68
– CD43
– CD33
– CD117
– Myeloperoxidase
– Lysozyme

12.5.2 Synonyms

Myeloid sarcoma is also known as chloroma (due to high myeloperoxidase content imparting a green color), granulocytic sarcoma (for tumors lacking a green color), or extramedullary myeloid tumor.

- Variably positive:
  - CD34
  - CD13
  - CD14
  - CD15
  - CD45
  - Antitrypsin
  - Antichymotrypsin
- Negative:
  - Pan B (CD20, CD19, CD79a) and T cell (CD3) markers
  - Melanocytic markers
  - Keratins
  - Muscle markers

12.5.3 Etiology

Myeloid sarcoma may be associated with acute myeloid leukemia, chronic myeloproliferative disorders, or no clinical evidence of hematologic disease.

12.5.4 Macroscopy

The cervix may be diffusely enlarged or nodular.

12.5.5 Microscopy

Myeloid sarcoma is composed of a diffuse proliferation of primitive, monotonous myeloid cells with medium to large, oval, irregular, reniform or folded nuclei, and fine chromatin, prominent nucleoli, and scant to moderate cytoplasm. Admixed maturing cells with recognizable myeloid differentiation may be seen, as well as lymphocytes, tingible body macrophages, and megakaryocytes [106–108]. Sclerosis and vascular wall involvement are common (Fig. 12.12). Rarely, pseudo-alveolar, trabecular, or cord-like patterns may be present.

Immunohistochemically, myeloid sarcoma is positive for CD68, CD43, CD33, CD117, myeloperoxidase, and lysozyme; variably positive for CD34, CD13, CD14, CD15, CD45, antitrypsin, and antichymotrypsin; negative for pan B (CD20, CD19, CD79a) and T cell (CD3) markers, melanocytic marker, keratins, and muscle markers.

Flow cytometry shows immature myeloid precursors. Genetic testing shows chromosomal aberrations in 55% of cases. One case of myeloid sarcoma confined to the cervix had a t(11;19)(q23;p13.3) involving the *MLL* and *ELL* genes [107].

Cytologically, the tumor cells exhibit scant cytoplasm and round to oval nuclei with finely dispersed chromatin. Cytoplasmic vacuoles may mimic signet ring cells.

Diagnostic Highlights

- Diffuse sheets of primitive monotonous myeloid cells
- Tumor cells with medium to large, oval, irregular, reniform or folded nuclei, fine chromatin, prominent nucleoli, and scant to moderate cytoplasm
- Admixed maturing cells with recognizable myeloid differentiation, lymphocytes, tingible body macrophages and megakaryocytes
- Sclerosis and vascular wall involvement
- Rarely, pseudo-alveolar, trabecular, or cord-like patterns

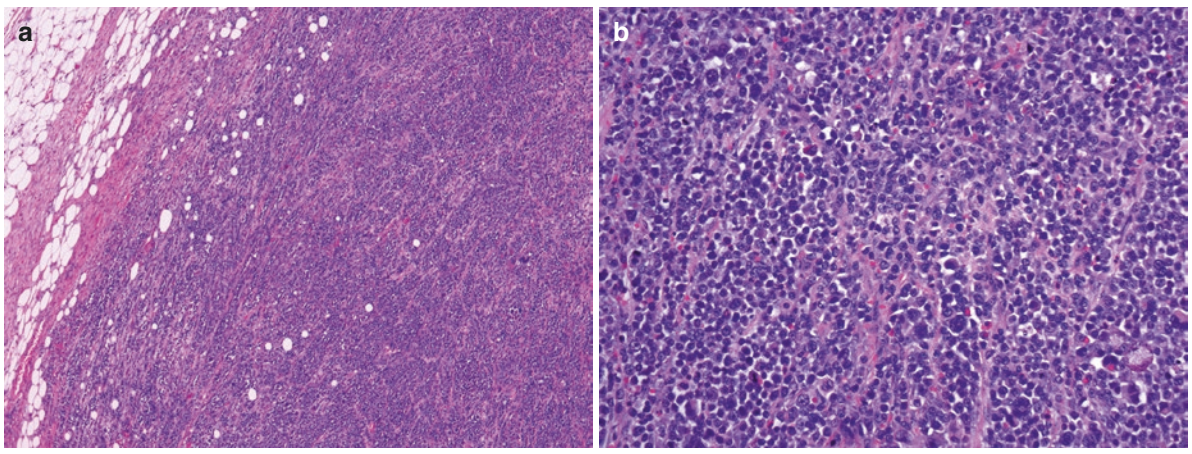

Fig. 12.12 Myeloid sarcoma. (**a–e**), Total hysterectomy with diffuse sheets of neoplastic cells involving the outer half of the cervical wall (H&E). The tumor cells exhibit large, oval, irregular, reniform or folded nuclei, fine chromatin, prominent nucleoli, and scant to moderate cytoplasm (**b–e**). Scattered megakaryocytes are seen (**d, e**). (**f–i**), Immunohistochemical stains show the tumor to be positive for CD34 (**f**), CD45 (**g**), myeloperoxidase (**h**), and CD117 (**i**). The patient has no prior history of hematologic disease

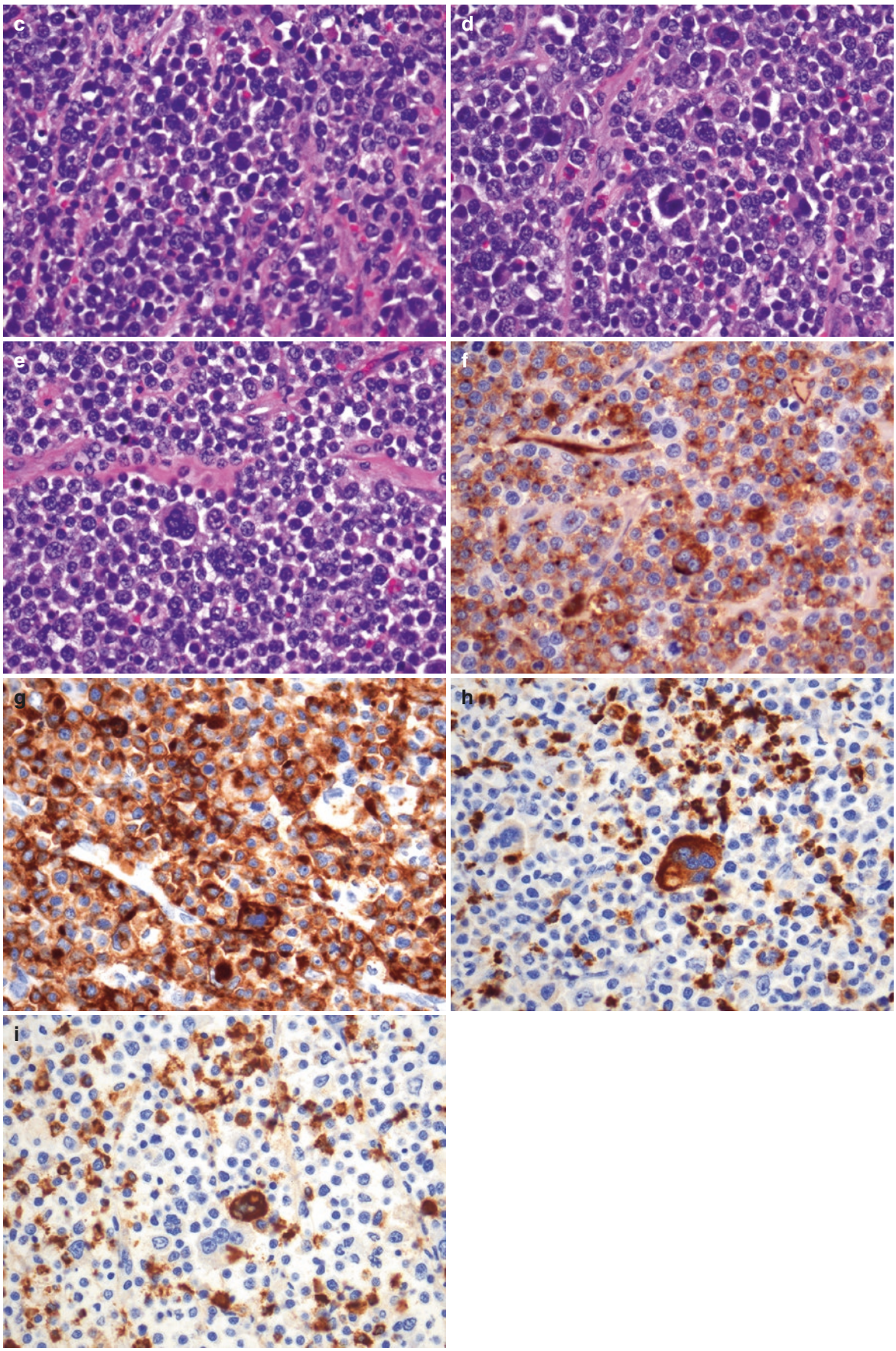

Fig. 12.12 (continued)

12.5.6 Differential Diagnosis

Same as lymphoid tumors (*see* Table 12.8).

12.5.7 Prognosis

Limited outcome data suggest that prognosis depends on the extent of disease and underlying genetic abnormalities [106, 107, 109].

References

1. Cid JM. Melanoid pigmentation of the endocervix: a neurogenic visceral argument. Ann Anat Pathol (Paris). 1959;4:617–28.
2. Goldman RL, Friedman NB. Blue nevus of the uterine cervix. Cancer. 1967;20:210–4.
3. Szumilo J, Patel A, Patel S, Burdan F. Blue nevus of the endocervix. Folia Morphol (Warsz). 2010;69:62–4.
4. Bhat ST, Shivamurthy A, Kini Rao AC. Incidentally detected blue nevus of endocervix: a case report. Iran J Pathol. 2015;10:248–52.
5. Owens OJ, Pollard K, Khoury GG, Dyson JE, Jarvis GJ, Joslin CA. Primary malignant melanoma of the uterine cervix. Clin Radiol. 1988;39:336–8.
6. Yu HC, Ketabchi M. Detection of malignant melanoma of the uterine cervix from Papanicolaou smears. A case report. Acta Cytol. 1987;31:73–6.
7. Feichter G, Curschellas E, Gobat S, Rickli J. Malignant melanoma of the uterine cervix; case report including cytology, histology and immunocytochemistry. Cytopathology. 1995;6:196–200.
8. Zamiati S, Sahraoui S, Jabri L, Louahlia S, Sqalli S, Kahlain A. Primary malignant melanoma of the cervix uteri: apropos of 1 case with review of the literature. Gynecol Obstet Fertil. 2001;29:381–5.
9. Pusceddu S, Bajetta E, Carcangiu ML, Formisano B, Ducceschi M, Buzzoni R. A literature overview of primary cervical malignant melanoma: an exceedingly rare cancer. Crit Rev Oncol Hematol. 2012;81:185–95.
10. Khoo US, Collins RJ, Ngan HY. Malignant melanoma of the female genital tract. A report of nine cases in the Chinese of Hong Kong. Pathology. 1991;23:312–7.
11. Rohwedder A, Philips B, Malfetano J, Kredentser D, Carlson JA. Vulvar malignant melanoma associated with human papillomavirus DNA: report of two cases and review of literature. Am J Dermatopathol. 2002;24:230–40.
12. Benson RJ, Tan LT. Radiation-induced malignant melanoma of the cervix. Clin Oncol (R Coll Radiol). 2000;12:234–7.
13. Deshpande AH, Munshi MM. Primary malignant melanoma of the uterine cervix: report of a case diagnosed by cervical scrape cytology and review of the literature. Diagn Cytopathol. 2001;25:108–11.
14. Srivastava P, Rath S, Hadi R, Husain N. Primary amelanotic malignant melanoma of cervix masquerading as squamous cell carcinoma presenting with extensive metastases. BMJ Case Rep. 2018;2018:bcr-2018-224723. https://doi.org/10.1136/bcr-2018-224723.
15. Mordel N, Mor-Yosef S, Ben-Baruch N, Anteby SO. Malignant melanoma of the uterine cervix: case report and review of the literature. Gynecol Oncol. 1989;32:375–80.
16. Furuya M, Shimizu M, Nishihara H, Ito T, Sakuragi N, Ishikura H, et al. Clear cell variant of malignant melanoma of the uterine cervix: a case report and review of the literature. Gynecol Oncol. 2001;80:409–12.
17. Pusceddu S, Bajetta E, Buzzoni R, Carcangiu ML, Platania M, Del Vecchio M, et al. Primary uterine cervix melanoma resembling malignant peripheral nerve sheath tumor: a case report. Int J Gynecol Pathol. 2008;27:596–600.
18. Norris HJ, Taylor HB. Melanomas of the vagina. Am J Clin Pathol. 1966;46:420–6.
19. Uzum N, Kose F, Ataoglu O. Metastatic malignant melanoma of the uterine cervix: first diagnosed on liquid-based cytology. Diagn Cytopathol. 2008;36:769–72.
20. Sugiyama VE, Chan JK, Shin JY, Berek JS, Osann K, Kapp DS. Vulvar melanoma: a multivariable analysis of 644 patients. Obstet Gynecol. 2007;110(2 Pt 1):296–301.
21. Tcheung WJ, Selim MA, Herndon JE 2nd, Abernethy AP, Nelson KC. Clinicopathologic study of 85 cases of melanoma of the female genitalia. J Am Acad Dermatol. 2012;67:598–605.
22. Chang SC, Chen CJ, Tseng HH. Primary malignant melanoma of the vagina and cervix uteri: case report and literature review. Zhonghua Yi Xue Za Zhi (Taipei). 1992;50:341–6.
23. Fleming H, Mein P. Primary melanoma of the cervix. A case report. Acta Cytol. 1994;38:65–9.
24. Stolnicu S, Szekely E, Molnar C, Molnar CV, Barsan I, D'Alfonso V, et al. Mature and immature solid teratomas involving uterine corpus, cervix, and ovary. Int J Gynecol Pathol. 2017;36:222–7.
25. Norris HJ, Zirkin HJ, Benson WL. Immature (malignant) teratoma of the ovary: a clinical and pathologic study of 58 cases. Cancer. 1976;37:2359–72.
26. O'Connor DM, Norris HJ. The influence of grade on the outcome of stage I ovarian immature (malignant) teratomas and the reproducibility of grading. Int J Gynecol Pathol. 1994;13:283–9.
27. Bell MC, Schmidt-Grimminger DC, Connor MG, Alvarez RD. A cervical teratoma with invasive squamous cell carcinoma in an HIV-infected patient: a case report. Gynecol Oncol. 1996;60:475–9.
28. Lim SC, Kim YS, Lee YH, Lee MS, Lim JY. Mature teratoma of the uterine cervix with lymphoid hyperplasia. Pathol Int. 2003;53:327–31.
29. Khorsandi F, Anabitarte M. Immature solid teratoma of the uterine cervix (author's transl). Geburtshilfe Frauenheilkd. 1981;41:347–9.
30. Iwanaga S, Ishii H, Nagano H, Shimizu M, Nishida T, Yakushiji M. Mature cystic teratoma of the uterine cervix. Asia Oceania J Obstet Gynaecol. 1990;16:363–6.
31. Young RH, Scully RE. Endodermal sinus tumor of the vagina: a report of nine cases and review of the literature. Gynecol Oncol. 1984;18:380–92.
32. Mardi K, Gupta N, Bindra R. Primary yolk sac tumor of cervix and vagina in an adult female: a rare case report. Indian J Cancer. 2011;48:515–6.
33. Copeland LJ, Sneige N, Ordonez NG, Hancock KC, Gershenson DM, Saul PB, et al. Endodermal sinus tumor of the vagina and cervix. Cancer. 1985;55:2558–65.
34. Chen SJ, Li YW, Tsai WY. Endodermal sinus (yolk sac) tumor of vagina and cervix in an infant. Pediatr Radiol. 1993;23:57–8.
35. Wang F, Liu A, Peng Y, Rakheja D, Wei L, Xue D, et al. Diagnostic utility of SALL4 in extragonadal yolk sac tumors: an immunohistochemical study of 59 cases with comparison to placental-like alkaline phosphatase, alpha-fetoprotein, and glypican-3. Am J Surg Pathol. 2009;33:1529–39.
36. Cao D, Liu A, Wang F, Allan RW, Mei K, Peng Y, et al. RNA-binding protein LIN28 is a marker for primary extragonadal germ cell tumors: an immunohistochemical study of 131 cases. Mod Pathol. 2011;24:288–96.
37. Mauz-Korholz C, Harms D, Calaminus G, Gobel U. Primary chemotherapy and conservative surgery for vaginal yolk-

sac tumour. Maligne Keimzelltumoren Study Group. Lancet. 2000;355(9204):625.
38. Rescorla F, Billmire D, Vinocur C, Colombani P, London W, Giller R, et al. The effect of neoadjuvant chemotherapy and surgery in children with malignant germ cell tumors of the genital region: a pediatric intergroup trial. J Pediatr Surg. 2003;38:910–2.
39. Tao T, Yang J, Cao D, Guo L, Chen J, Lang J, et al. Conservative treatment and long-term follow up of endodermal sinus tumor of the vagina. Gynecol Oncol. 2012;125:358–61.
40. Longo R, Battaglia F, Gattuso D, De Sio L, Sarmiento R, Amici S, et al. Primary nongestational choriocarcinoma of the uterine cervix. J Clin Oncol. 2011;29:e301–2.
41. Maesta I, Michelin OC, Traiman P, Hokama P, Rudge MV. Primary non-gestational choriocarcinoma of the uterine cervix: a case report. Gynecol Oncol. 2005;98:146–50.
42. Hwang DW, Song HS, Choi YY, Kim HS, Kim YA, Chun KC. Primary non-gestational choriocarcinoma of the uterine cervix with metaplastic transformation from adenocarcinoma: a case report. J Obstet Gynaecol. 2018;38:289–90.
43. Mukonoweshuro P, McCluggage WG. Clear cell carcinoma of the cervix with choriocarcinomatous differentiation: report of an extremely rare phenomenon associated with mismatch repair protein abnormality. Int J Gynecol Pathol. 2017;36:323–7.
44. Lurain JR, Brewer JI, Torok EE, Halpern B. Natural history of hydatidiform mole after primary evacuation. Am J Obstet Gynecol. 1983;145:591–5.
45. Baykal C, Tulunay G, Bulbul D, Boran N, Kose MF. Primary choriocarcinoma of the uterine cervix in a postmenopausal patient: a case report. Gynecol Oncol. 2003;90:667–9.
46. Seckl MJ, Fisher RA, Salerno G, Rees H, Paradinas FJ, Foskett M, et al. Choriocarcinoma and partial hydatidiform moles. Lancet. 2000;356(9223):36–9.
47. Savage J, Adams E, Veras E, Murphy KM, Ronnett BM. Choriocarcinoma in women: analysis of a case series with genotyping. Am J Surg Pathol. 2017;41:1593–606.
48. Koo HL, Choi J, Kim KR, Kim JH. Pure non-gestational choriocarcinoma of the ovary diagnosed by DNA polymorphism analysis. Pathol Int. 2006;56:613–6.
49. Morgan JM, Lurain JR. Gestational trophoblastic neoplasia: an update. Curr Oncol Rep. 2008;10:497–504.
50. Seckl MJ, Sebire NJ, Fisher RA, Golfier F, Massuger L, Sessa C. Gestational trophoblastic disease: ESMO clinical practice guidelines for diagnosis, treatment and follow-up. Ann Oncol. 2013;24(Suppl 6):vi39–50.
51. Mitrovic S, Arsenijevic PS, Kljakic D, Djuric JM, Milosavljevic MZ, Protrka ZM, et al. Gestational choriocarcinoma of the cervix. Arch Iran Med. 2014;17:783–5.
52. Kairi-Vassilatou E, Papakonstantinou K, Grapsa D, Kondi-Paphiti A, Hasiakos D. Primary gestational choriocarcinoma of the uterine cervix. Report of a case and review of the literature. Int J Gynecol Cancer. 2007;17:921–5.
53. Horn LC, Bilek K, Nenning H. Postpartal gestational choriocarcinoma fatally misdiagnosed as squamous cell cancer of the uterine cervix. Gen Diagn Pathol. 1997;143:191–6.
54. Park M, Han SS, Lee EJ, Byon M, Kim MY, Kim MK, et al. Primary cervical choriocarcinoma during viable intrauterine pregnancy. J Obstet Gynaecol Res. 2015;41:1291–4.
55. Kurman RJ, Scully RE, Norris HJ. Trophoblastic pseudotumor of the uterus: an exaggerated form of "syncytial endometritis" simulating a malignant tumor. Cancer. 1976;38:1214–26.
56. Hui P. Gestational trophoblastic tumors: a timely review of diagnostic pathology. Arch Pathol Lab Med. 2019;143:65–74.
57. Baergen RN, Rutgers JL, Young RH, Osann K, Scully RE. Placental site trophoblastic tumor: a study of 55 cases and review of the literature emphasizing factors of prognostic significance. Gynecol Oncol. 2006;100:511–20.
58. Shih IM. Trophogram, an immunohistochemistry-based algorithmic approach, in the differential diagnosis of trophoblastic tumors and tumorlike lesions. Ann Diagn Pathol. 2007;11:228–34.
59. Takekawa Y, Yamamoto T, Sakakibara M, Kimura M, Yoshii R, Yamashita Y. Cytologic findings of epithelioid trophoblastic tumor of the uterus: a case report. Acta Cytol. 2010;54:345–8.
60. Kamoi S, Ohaki Y, Mori O, Yokoyama M, Kawamoto Y, Kawamura T, et al. Epithelioid trophoblastic tumor of the uterus: cytological and immunohistochemical observation of a case. Pathol Int. 2002;52:75–81.
61. Papadopoulos AJ, Foskett M, Seckl MJ, McNeish I, Paradinas FJ, Rees H, et al. Twenty-five years' clinical experience with placental site trophoblastic tumors. J Reprod Med. 2002;47:460–4.
62. Schmid P, Nagai Y, Agarwal R, Hancock B, Savage PM, Sebire NJ, et al. Prognostic markers and long-term outcome of placental-site trophoblastic tumours: a retrospective observational study. Lancet. 2009;374:48–55.
63. Silva EG, Tornos C, Lage J, Ordonez NG, Morris M, Kavanagh J. Multiple nodules of intermediate trophoblast following hydatidiform moles. Int J Gynecol Pathol. 1993;12:324–32.
64. Jones WB, Romain K, Erlandson RA, Burt ME, Lewis JL Jr. Thoracotomy in the management of gestational choriocarcinoma. A clinicopathologic study. Cancer. 1993;72:2175–81.
65. Mazur MT. Metastatic gestational choriocarcinoma. Unusual pathologic variant following therapy. Cancer. 1989;63:1370–7.
66. Shih IM, Kurman RJ. The pathology of intermediate trophoblastic tumors and tumor-like lesions. Int J Gynecol Pathol. 2001;20:31–47.
67. Shih IM. Gestational trophoblastic neoplasia--pathogenesis and potential therapeutic targets. Lancet Oncol. 2007;8:642–50.
68. Narita F, Takeuchi K, Hamana S, Ohbayashi C, Ayata M, Maruo T. Epithelioid trophoblastic tumor (ETT) initially interpreted as cervical cancer. Int J Gynecol Cancer. 2003;13:551–4.
69. Tsai HW, Lin CP, Chou CY, Li CF, Chow NH, Shih IM, et al. Placental site nodule transformed into a malignant epithelioid trophoblastic tumour with pelvic lymph node and lung metastasis. Histopathology. 2008;53:601–4.
70. Chen BJ, Cheng CJ, Chen WY. Transformation of a post-cesarean section placental site nodule into a coexisting epithelioid trophoblastic tumor and placental site trophoblastic tumor: a case report. Diagn Pathol. 2013;8:85.
71. Fadare O, Parkash V, Carcangiu ML, Hui P. Epithelioid trophoblastic tumor: clinicopathological features with an emphasis on uterine cervical involvement. Mod Pathol. 2006;19:75–82.
72. Shih IM, Kurman RJ. Epithelioid trophoblastic tumor: a neoplasm distinct from choriocarcinoma and placental site trophoblastic tumor simulating carcinoma. Am J Surg Pathol. 1998;22:1393–403.
73. Lurain JR. Gestational trophoblastic disease II: classification and management of gestational trophoblastic neoplasia. Am J Obstet Gynecol. 2011;204:11–8.
74. Mandato VD, Palermo R, Falbo A, Capodanno I, Capodanno F, Gelli MC, et al. Primary diffuse large B-cell lymphoma of the uterus: case report and review. Anticancer Res. 2014;34:4377–90.
75. Upanal N, Enjeti A. Primary lymphoma of the uterus and cervix: two case reports and review of the literature. Aust N Z J Obstet Gynaecol. 2011;51:559–62.
76. Dursun P, Gultekin M, Bozdag G, Usubutun A, Uner A, Celik NY, et al. Primary cervical lymphoma: report of two cases and review of the literature. Gynecol Oncol. 2005;98:484–9.
77. Van Renterghem N, De Paepe P, Van den Broecke R, Bourgain C, Serreyn R. Primary lymphoma of the cervix uteri: a diagnostic challenge. Report of two cases and review of the literature. Eur J Gynaecol Oncol. 2005;26:36–8.

78. Vang R, Medeiros LJ, Ha CS, Deavers M. Non-Hodgkin's lymphomas involving the uterus: a clinicopathologic analysis of 26 cases. Mod Pathol. 2000;13:19–28.
79. Zannoni GF, Vellone VG, Petrillo M, Fadda G, Rossi ED, Scambia G, et al. Secondary malignancies of the uterine cervix: a potential diagnostic pitfall. Virchows Arch. 2013;463:23–9.
80. Winer N, Maisonneuve H, Magois C, Sagot P, Lopes P, Boog G, et al. Malignant non-Hodgkin's lymphoma of the cervix. A case report. J Gynecol Obstet Biol Reprod (Paris). 1995;24:25–9.
81. Pec J Jr, Pecova K, Pec J Sr, Plank L, Homola A, Lazarova Z. A study of possible causal relations between squamous cell carcinoma of the penis and carcinoma of the cervix uteri. Int Urol Nephrol. 1992;24:313–7.
82. Strang P, Sorbe B, Sundstrom C. Primary aneuploid lymphoma of the uterine cervix: a case report. Gynecol Oncol. 1988;30:302–5.
83. Stein L. Chronic lymphatic leukaemia presenting as neoplasm of the cervix uteri. J Obstet Gynaecol Br Emp. 1949;56:107.
84. Mainiero A, Schnatz PF. Chronic lymphocytic leukemia presenting with localized gynecologic symptoms. J Low Genit Tract Dis. 2010;14:63–4.
85. Barcos M, Lane W, Gomez GA, Han T, Freeman A, Preisler H, et al. An autopsy study of 1206 acute and chronic leukemias (1958 to 1982). Cancer. 1987;60:827–37.
86. Mikhail MS, Runowicz CD, Kadish AS, Romney SL. Colposcopic and cytologic detection of chronic lymphocytic leukemia. Gynecol Oncol. 1989;34:106–8.
87. Mikami Y, Maehata K, Fujiwara K, Sasano H. Squamous cell carcinoma of the uterine cervix in association with stage 0 chronic lymphocytic leukemia/small lymphocytic lymphoma. Gynecol Oncol. 2004;92:974–7.
88. Magley J, Moyers C, Ballard KS, Tedjarati S. Secondary cervical cancer in a patient with chronic lymphocytic leukemia and recurrent chronic lymphocytic leukemia mimicking recurrent cervical dysplasia: a case report. J Reprod Med. 2010;55:175–8.
89. Udupa K, Ganesan P, Majhi U, Sagar TG. Unusual involvement of cervix and vulva in a case of chronic lymphocytic leukemia. J Gynecol Oncol. 2012;23:205–6.
90. Vang R, Medeiros LJ, Fuller GN, Sarris AH, Deavers M. Non-Hodgkin's lymphoma involving the gynecologic tract: a review of 88 cases. Adv Anat Pathol. 2001;8:200–17.
91. Kosari F, Daneshbod Y, Parwaresch R, Krams M, Wacker HH. Lymphomas of the female genital tract: a study of 186 cases and review of the literature. Am J Surg Pathol. 2005;29:1512–20.
92. Rossi G, Bonacorsi G, Longo L, Artusi T, Rivasi F. Primary high-grade mucosa-associated lymphoid tissue-type lymphoma of the cervix presenting as a common endocervical polyp. Arch Pathol Lab Med. 2001;125:537–40.
93. Li WS, Wang RC, Wang J, Chang KC. Primary nodular lymphocyte-predominant Hodgkin lymphoma of uterine cervix mimicking leiomyoma. Clin Case Rep. 2015;3:349–52.
94. Lovell MO, Valente PT. Unique collision of Hodgkin lymphoma and adenosquamous carcinoma in the uterine cervix: synchronous malignant neoplasms of the cervix. J Low Genit Tract Dis. 2003;7:307–10.
95. Harris NL, Scully RE. Malignant lymphoma and granulocytic sarcoma of the uterus and vagina. A clinicopathologic analysis of 27 cases. Cancer. 1984;53:2530–45.
96. Chan JK, Loizzi V, Magistris A, Hunter MI, Rutgers J, DiSaia PJ, et al. Clinicopathologic features of six cases of primary cervical lymphoma. Am J Obstet Gynecol. 2005;193:866–72.
97. Chandy L, Kumar L, Dawar R. Non-Hodgkin's lymphoma presenting as a primary lesion in uterine cervix: case report. J Obstet Gynaecol Res. 1998;24:183–7.
98. Garavaglia E, Taccagni G, Montoli S, Panacci N, Ponzoni M, Frigerio L, et al. Primary stage I-IIE non-Hodgkin's lymphoma of uterine cervix and upper vagina: evidence for a conservative approach in a study on three patients. Gynecol Oncol. 2005;97:214–8.
99. Lagoo AS, Robboy SJ. Lymphoma of the female genital tract: current status. Int J Gynecol Pathol. 2006;25:1–21.
100. Carbone A, Gloghini A, Libra M, Gasparotto D, Navolanic PM, Spina M, et al. A spindle cell variant of diffuse large B-cell lymphoma possesses genotypic and phenotypic markers characteristic of a germinal center B-cell origin. Mod Pathol. 2006;19:299–306.
101. Kahlifa M, Buckstein R, Perez-Ordonez B. Sarcomatoid variant of B-cell lymphoma of the uterine cervix. Int J Gynecol Pathol. 2003;22:289–93.
102. Bagg A. Role of molecular studies in the classification of lymphoma. Expert Rev Mol Diagn. 2004;4:83–97.
103. Cohn DE, Resnick KE, Eaton LA, de Hart J, Zanagnolo V. Non-Hodgkin's lymphoma mimicking gynecological malignancies of the vagina and cervix: a report of four cases. Int J Gynecol Cancer. 2007;17:274–9.
104. Dominis M, Dzebro S, Gasparov S, Pesut A, Kusec R. Diffuse large B-cell lymphoma and its variants. Croat Med J. 2002;43:535–40.
105. Hans CP, Weisenburger DD, Greiner TC, Gascoyne RD, Delabie J, Ott G, et al. Confirmation of the molecular classification of diffuse large B-cell lymphoma by immunohistochemistry using a tissue microarray. Blood. 2004;103:275–82.
106. Garcia MG, Deavers MT, Knoblock RJ, Chen W, Tsimberidou AM, Manning JT Jr, et al. Myeloid sarcoma involving the gynecologic tract: a report of 11 cases and review of the literature. Am J Clin Pathol. 2006;125:783–90.
107. Ouansafi I, Arabadjief M, Mathew S, Srivastara S, Orazi A. Myeloid sarcoma with t(11;19)(q23;p13.3) (MLL-ELL) in the uterine cervix. Br J Haematol. 2011;153:679.
108. Oliva E, Ferry JA, Young RH, Prat J, Srigley JR, Scully RE. Granulocytic sarcoma of the female genital tract: a clinicopathologic study of 11 cases. Am J Surg Pathol. 1997;21:1156–65.
109. Kamboj M, Sharma A, Gupta G, Pasricha S. Isolated myeloid sarcoma of cervix: Aleukemic presentation. J Cancer Res Ther. 2017;13:1076–7.